Heterogeneous potential of human airway basal cells: Holoclone-stem cell identification in a clinical-grade system

Adamo Davide[1,4†]*, Genna Vincenzo Giuseppe[1,2†], Galaverni Giulia[1,4], Chiavelli Chiara[1,3], Merra Alessia[1,4], Lepore Fabio[1,3], Boraldi Federica[4], Quaglino Daniela[4], Evangelista Jessica[5,6], Lococo Filippo[5,6], Pellegrini Graziella[1, 2,4]*.

[1]Centre for Regenerative Medicine "Stefano Ferrari", University of Modena and Reggio Emilia, Modena, Italy.
[2] Holostem Terapie Avanzate S.r.l., Modena, Italy
[3] Department of Oncology and Hematology, Azienda Ospedaliero-Universitaria di Modena, Modena, Italy
[4]Department of Life Sciences, University of Modena and Reggio Emilia, Modena, Italy.
[5] Thoracic Surgery Unit, Fondazione Policlinico Universitario A. Gemelli IRCCS, Rome, Italy.
[6] Università Cattolica del Sacro Cuore, Rome, Italy.

*Corresponding authors
E-mail: davide.adamo@unimore.it (D.A.)
E-mail: graziella.pellegrini@unimore.it (G.P.)
[†]These authors contributed equally to this work.

GRAPHICAL ABSTRACT

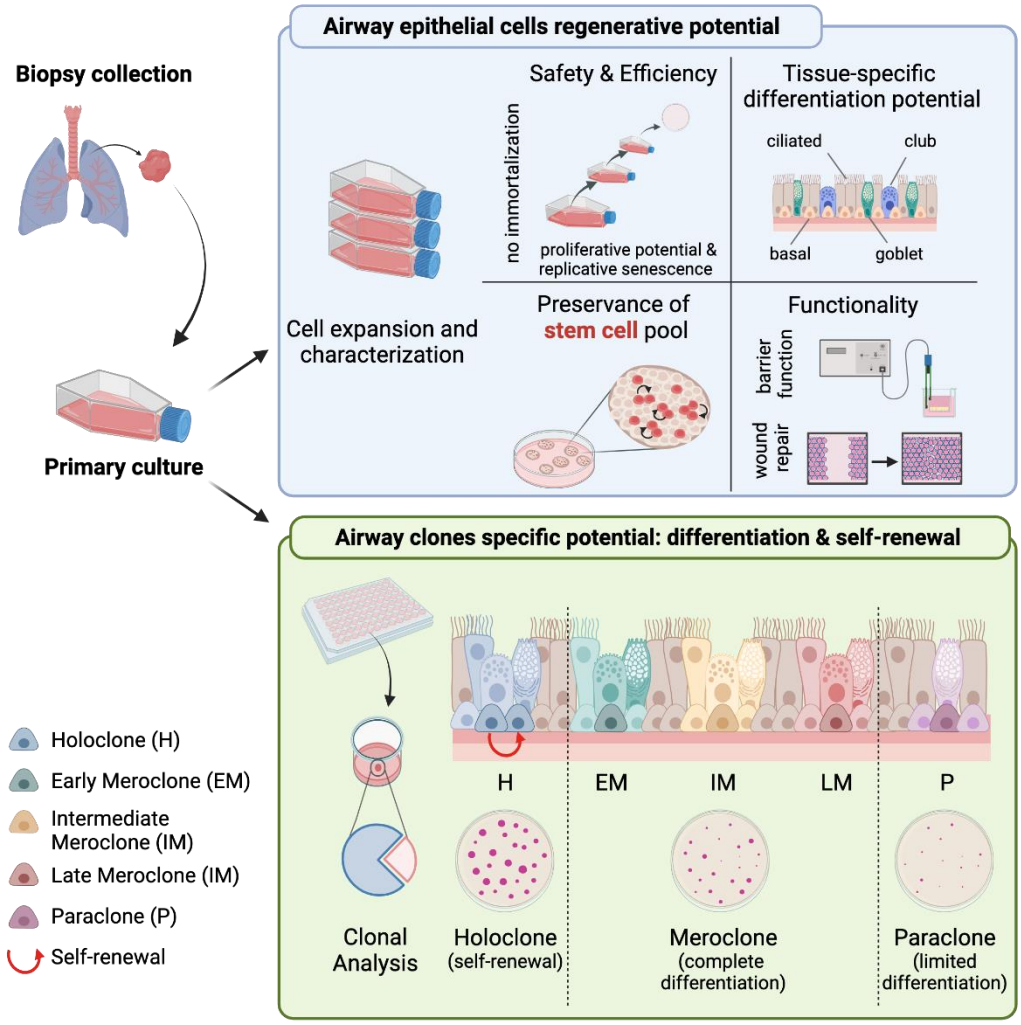

ABSTRACT

The clinical results of tissue engineering approaches aimed at treating extensive tracheal or bronchial defects highlighted some impactful limitations, among which stand out the inability to regenerate a functional and self-renewing airway epithelium onto the bioengineered graft. This outcome is often caused by culture conditions unable to sustain the long-term proliferative and differentiative potential of primary airway epithelial cells, resulting in progressive stem cell exhaustion. Here, we examined the capacity of a clinical-grade culture system to safely and efficiently support the *in vitro* expansion of primary human tracheal and bronchial epithelial cells, regenerating a functional and fully differentiated airway epithelium. Moreover, we identified and characterized airway epithelial stem cells, unravelling the mechanisms that underlie tracheobronchial epithelium renewal. Finally, we suggested possible parameters to be employed as quality controls during critical stages of the tissue engineering process, thereby maximizing the likelihood of success of the treatment and prioritizing patients' safety, crucial prerequisites before embarking on other clinical applications.

KEYWORDS

Tracheobronchial epithelium, epithelial stem cells, airway holoclone, regenerative medicine, tissue engineering, airway reconstruction, respiratory mucosa; clinical-grade expansion, airway differentiation, stem cell markers.

INTRODUCTION

The respiratory system is one of the most important and intricate systems within our body [1,2]. However, a variety of pathological conditions such as malignancies, congenital malformations, infections, inflammations, or postoperative complications can deeply alter its functions, endangering the patients' life [3–7]. Over the years, extensive circumferential tracheal or bronchial damages have posed a significant challenge in airway medicine [8,9]. In such cases, conventional surgical approaches proved ineffective, highlighting the pressing demand for innovative reconstructive strategies [10–13]. Tissue engineering (TE) has been investigated as a promising solution for damaged or pathological airway tissue replacement [5,14–16]. However, the clinical outcomes of these applications highlighted some impactful limitations, including difficulties in identifying a supporting biomaterial with appropriate biomechanical properties [11,13,17,18], immune-rejection risks [19], delayed revascularization of the bioengineered graft [20] and inability to regenerate a functional and self-renewing airway epithelium onto the engineered implant [8,21–23]. Specifically, the respiratory epithelium plays a critical role in airway functions, and its absence leads to numerous complications, such as mucus buildup, infections, graft stenosis, granulation tissue formation, chondromalacia, and fibrogenic reactions [8,21,23,24]. To fulfil its functions, the respiratory epithelium comprises various primary cell populations, including basal, goblet, club and ciliated cells, along with several less abundant cell types, collectively accounting for 0.8% of the total airway epithelium composition [25]. The first problem encountered in TE airway epithelial regeneration is efficiently expanding primary cells to the extent required for transplantation while maintaining their inherent heterogeneity [26–28]. Indeed, preclinical studies describing airway epithelial cell *in vitro* cultivation, generally reported a slow cell growth rate [23] and a minimal proliferative potential, with a very limited number of subculturing passages [29]. Beyond this limit, they lose their capacity to proliferate, differentiate, produce mucus, and express tight junction proteins [30–32]. Consequently, autologous airway epithelial cells are reported to be inadequate for clinical regeneration needs and an unsuitable and unreliable cell source for TE approaches [23]. In addition to promptly achieving an effective *ex vivo* expansion, as required in urgent cases of life-saving reconstructions [33], the maintenance of the epithelial stem cell population is of utmost importance. This preservation should be assured in all stages of the engineering process, starting from biopsy collection and cell extraction to the *in vitro* expansion and graft repopulation, ending with a defined revascularization strategy that should ensure sufficient blood supply to the transplanted tissue [8,10,32]. Indeed, successful clinical applications of regenerative medicine unveiled that the permanent engraftment and long-term regeneration of transplanted epithelial tissues critically depend on having a sufficient number of stem cells [34–37]. Hence, it becomes crucial to identify specific biological parameters that can unequivocally determine the quality of the epithelial culture [38–41]. Here, we examined the capacity of a clinical-grade culture system [34,42–44] to achieve a

safe, efficient, and rapid expansion of human primary airway tracheal (AT) and bronchial (AB) epithelial cells while preserving their tissue-specific heterogeneity.
Our primary focus was to identify and characterize airway epithelial stem cells, suggesting quality controls to be performed throughout the bioengineering procedure and posing the basis for new methods to prospectively identify stem cells within airway cultures.
Additionally, we delved into the mechanisms governing AT and bronchial AB epithelial cells differentiation and specialization, unravelling the role of stem and progenitor cells in maintaining airway epithelia heterogeneity. The increased understanding of tissue-specific biology and its regenerative potential under *in vitro* expansion can address critical hurdles in airway tissue engineering, thereby promoting successful translational research.

RESULTS

In Vivo Characterization of Human Airway Tissues

We first assessed the native expression and localization of relevant epithelial markers *in vivo* using freshly collected tracheal and bronchial human biopsies as a reference for the subsequent *in vitro* analyses and to check the integrity of the starting biopsy (**Figure S1A, B**). According to published data [45], airway tissue sections from both districts showed a predominantly basal expression of cytokeratin (CK) 5 and CK14 and a widespread expression of CK18 and CK19 throughout the epithelium (**Figure S1A, B**). We also confirmed the presence of the principal specialized cell types of the airway epithelium, namely ciliated cells (Acetylated Tubulin-positive cells), goblet cells (Mucin5AC-positive) and club cells (Uteroglobin-positive), indicative of physiological epithelial complexity and functionality (**Figure S1B**). Furthermore, the apical side of the airway epithelium, negative for Involucrin staining, was characterized by a dense network of zonula occludens-1 (ZO-1) positive tight junctions highlighting the epithelial integrity and its fundamental role as a physical barrier (**Figure S1B**). The analysis of the mitotic cell marker Ki-67 revealed the presence of only a few actively proliferating cells, coherent with a slow turn-over rate [46], showing a predominant suprabasal localization and a slightly higher abundance in the tracheal samples compared to the bronchial ones (**Figure S1A**). Conversely, cells expressing the alpha isoform of the epithelial stem-progenitor cell marker p63 (p63α) were mainly located in the basal layer (**Figure S1A**).

Clonogenic and Proliferative Potential of Human Airway Primary Cultures

The long-term proliferative and differentiative potentials of AT and AB epithelial cells were evaluated through a clinically validated cell culture system, consisting of growing primary epithelial cells on a lethally irradiated feeder layer of certified 3T3-J2 cells. Firstly, pioneered by Rheinwald and Green [47], this system is well-reckoned as the standard method for the *ex vivo* expansion and clinical application of many epithelial tissues [35,41,44,48,49] but has never been efficiently employed for human airway epithelial cells.
In the expansion after cell isolation, the colony-forming efficiency (CFE) assay revealed an increased percentage of clonogenic cells in AT (58.87 ± 14%) and AB (66.23 ± 24%) primary cultures compared to that of cells directly isolated from the biopsy, whose clonogenicity was quantified as 13.37 ± 11% (AT) and 10.87% ± 5% (AB) (**Figure 1A, B**). This increase highlights the culture system's capacity to selectively sustain epithelial cell growth over other cell types and to support the expansion of cells with the highest proliferative potential, while those terminally differentiated undergo replicative senescence.
Then, to evaluate the long-term proliferative potential of human airway epithelial cells, we sub-cultivated three AT and AB independent human primary cultures (strains) for serial passages up to replicative senescence. All the cultures displayed an extensive proliferative potential, with AT cells performing between 27 and 44 passages (**Figure 1C**) and AB cells between 24 and 28 passages (**Figure 1C**). Native cellular biology was preserved without any immortalization events being registered, as desirable for expanding primary cells in a clinical setting. Indeed, the progressive decrease in clonogenic cells of AT and AB strains during the serial passages, coupled with an increasingly higher percentage of colonies made of large, terminally differentiated cells, scored as aborted colonies (**Figure 1A, B, C**), proved the physiologic advancement of proliferative senescence. (**Figure 1C, D**).
The growth potential of airway epithelial cells was also assessed through their ability to produce cell doublings (c.d.), calculated as 216 ± 52 c.d. and 161 ± 16 c.d. respectively for AT and AB epithelial cells (**Figure 1E**). The doubling time was in line with other human cultured epithelia [50]: AT strains took 35 ± 19.4 hours to

duplicate, while 20 ± 0.8 hours were necessary for AB strains. No significant differences were recorded for cell doublings and doubling time between the two districts (**Figure 1E**).

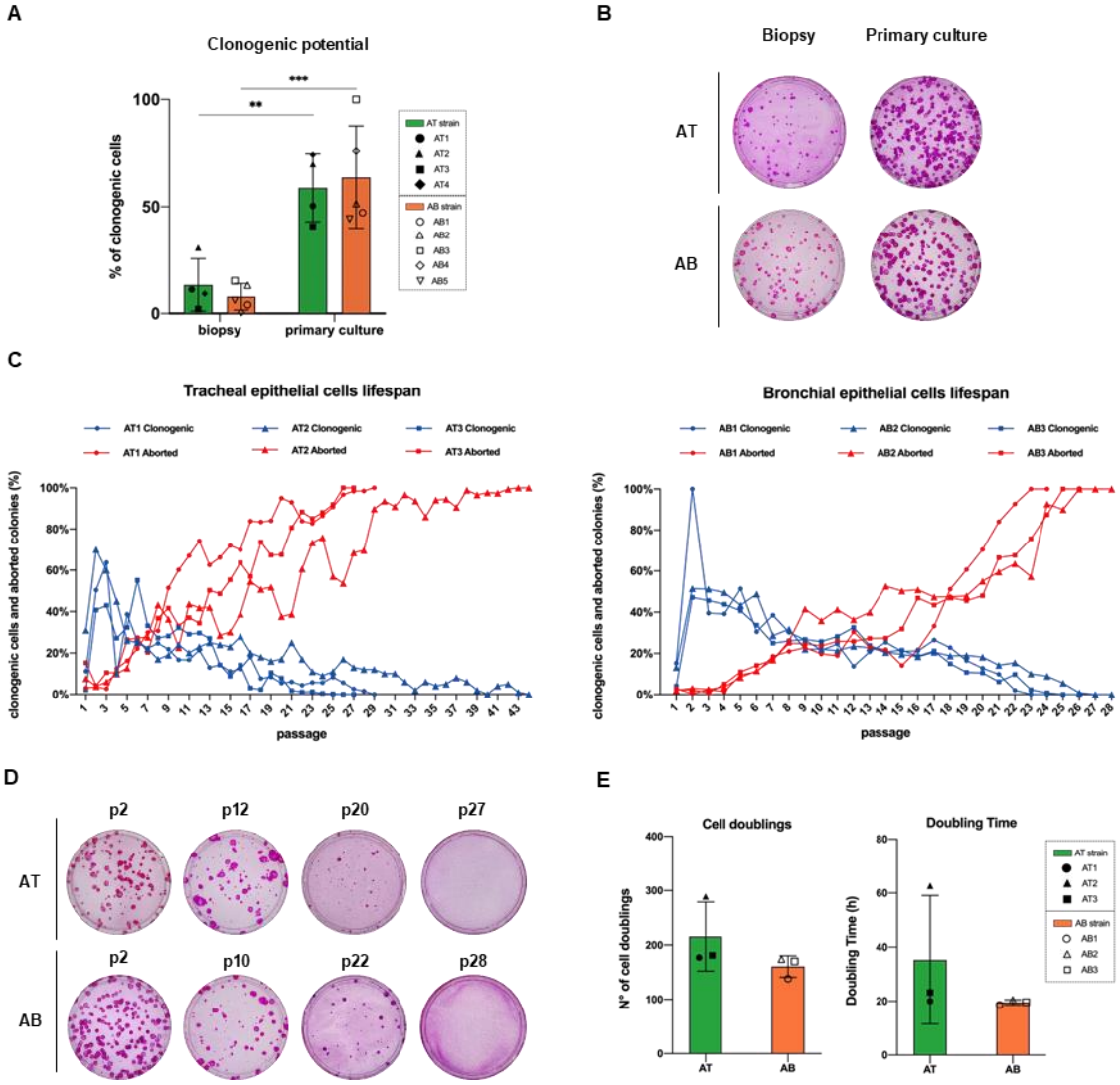

Figure 1. Cell Extraction and Long-term Proliferative Potential of Primary Human Airway Epithelial Cells
(A) Comparison between the clonogenicity of cells directly extracted from AT (n = 4) and AB (n = 5) biopsies and after the first expansion passage. Each independent strain is indicated with a different shape. Unpaired, biparametric, two-tailed t test.
(B) Representative images of CFE assay performed at cell extraction (biopsy, 1000 cells seeded) and after one passage of cell propagation (p1, 400 cells seeded).
(C) Graphs showing the quantification of CFE assay during AT culture lifespans (left, n = 3) and AB culture lifespans (right, n = 3). Blue lines indicate the percentage of clonogenic cells (number of colonies/total seeded cells ratio); red lines indicate the percentage of aborted colonies (aborted colonies/total grown colonies ratio). Independent human strains are indicated with different shapes.
(D) Representative images of CFE indicator dishes showing clonogenic and aborted colonies trends in AT3 and AB2 lifespans. The number of cells seeded in AT3 serial passages is 300 (p2), 500 (p12), 2000 (p20), 67,000 (p27); number of cells seeded in AB2 serial passages is 400 (p2), 600 (p10), 700 (p22), 250,000 (p28).
(E) Histograms showing the cell doublings (left) and doubling time (right) of AT (n = 3, green bar) and AB (n = 3, orange bar) independent strains, indicated with different shapes. Unpaired, biparametric, two-tailed t test. Values are shown as mean ± SD. ***$p < 0.001$, **$p < 0.01$.

Airway Epithelial Cell Culture Characterization

From the perspective of future clinical applications involving *in vitro* expanded human primary cells, the cell culture characterization allows *(i)* to understand the culture system's impact on cellular physiology, *(ii)* to identify and master variables, and *(iii)* to define appropriate quality controls. Therefore, we analyzed the expression of critical epithelial markers during airway cells lifespan through immunofluorescence (IF) staining and western blot (WB) analysis. The stable expression of CK5 and CK14, preferentially detected into tracheal and bronchial epithelia' basal layer (**Figure S1**), revealed airway cultured cells preserving both their basal origin and epithelial nature throughout the expansion procedure (**Figure 2A, S2A**). Consistently with *in vivo* results, CK18 was expressed by all expanded AT and AB epithelial cells (**Figure S2A**). The analysis of Involucrin (**Figure 2A**) and 14-3-3-sigma (or stratifin, **Figure S2A**), early epithelial differentiation markers, revealed the ability of the culture system to support physiological cell differentiation. Of note, Involucrin, barely detectable in the native tissue (**Figure S1**), appeared expressed by the most stratified cells within the growing colonies (**Figure 2A**). Further, the close network of ZO-1 positive tight junctions revealed each colony as a well-organized piece of tissue, suggesting the regeneration of an epithelium endowed with a barrier function (**Figure 2A).** Ultimately, in accordance with the progressive reduction of clonogenic cells (**Figure 1C**), we observed a decrease in the number of cells positively stained for the proliferative marker Ki-67 and the stem/progenitor cell marker p63α along the culture's lifespan (**Figure 2A, S2A**).

In order to further integrate these data and evaluate additional markers, we performed a WB analysis at five different time points of human epithelial cultures (see "Star Methods"). Consistently with IF analysis, CK14 and Involucrin were almost stably expressed throughout the serial passages of AT and AB lifespans, with no significant differences reported (**Figure 2B, C**). Additionally, the analysis of the three transcriptional factors (TFs) p63α, BMI1 and SOX2 – involved in stem cell function regulation [51–55] – revealed them as significantly more expressed in the first expansion passages (time points I and II, enriched in stem-progenitor cells) rather than at the end of the cultures' lifespan (time point V) (**Figure 2B, C**). The progressive decrease of these TFs, observed in all AT and AB strains, corroborates the hypothesis of a possible correlation with the stem-progenitor cell population.

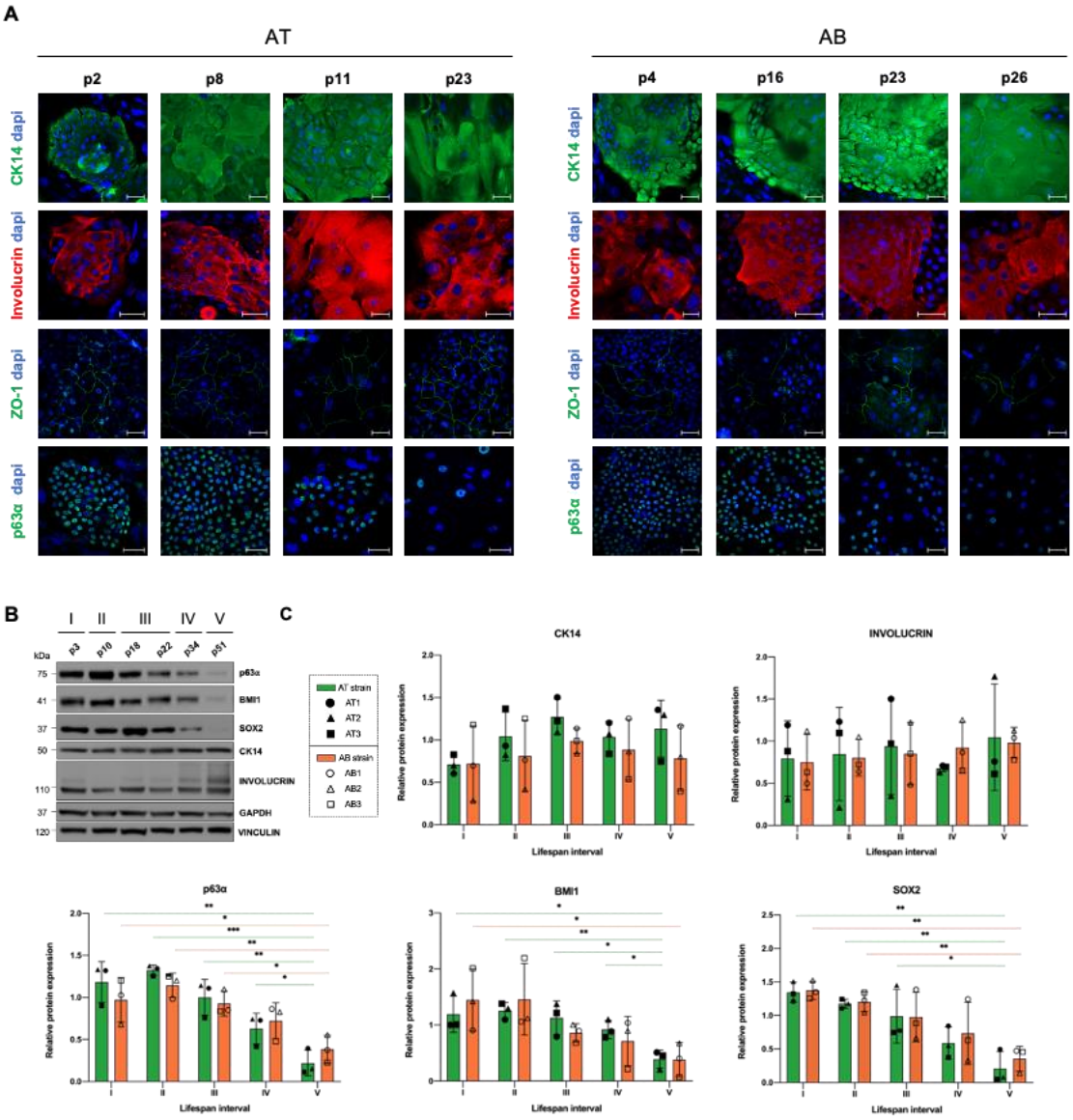

Figure 2. Characterization of Airway Epithelial Cell Cultures

(A) IF staining of AT (left) and AB (right) cultures at four different time points of airway epithelial cell lifespan (representative images of n = 3 AT and n = 3 AB primary human independent strains). Scale bars, 50 µm.

(B) WB analysis on total cell extracts from six expansion passages (AT2 strain) representative of five consecutive lifespan intervals, immunostained with indicated antibodies. Experiment conducted on n = 3 AT strains (n = 5 technical replicates) and n = 3 AB strains (n = 4 technical replicates).

(C) Histograms showing the quantification of the expression levels from top left to bottom right of CK14, Involucrin, p63α, BMI1 (all normalized per GAPDH) and SOX2 (normalized per Vinculin). Average and SD of n = 3 AT and n = 3 AB displayed per each time range (see "Star Methods"). Independent strains are indicated with different shapes. Unpaired, biparametric, two-tailed t test *p < 0.05.; ** p < 0.01 and *** p < 0.001.

Long-term Regenerative and Differentiative Potential of Tracheobronchial Epithelial Cells

Together with extensive proliferative potential, the preservation of the peculiar airway cellular heterogeneity is a crucial feature in expanding epithelial cells for a tissue-engineering approach. Hence, we tested the presence of specialized MUC5AC-positive goblet and Uteroglobin-positive club cells during airway epithelial cell lifespans. Both goblet and club cells were detected in all AT and AB cultures, proving the culture system's ability to sustain the tissue-specific differentiative potential of airway cultures **(Figure 3A, B, S2B)**. Furthermore, the adopted clinical-grade culture conditions allowed to explicit the biological variability among independent human strains, as reflected by the fluctuation in the abundance of differentiated cells observed during the cultures' lifespan (**Figure 3B**). Despite this physiological variability, a distinct trend in the appearance of differentiated cells was clearly visible. Indeed, AB strains presented both club and goblet cells

since the very early expansion passages**,** while AT strains showed a significant number of these specialized cell populations only later in the expansion procedure **(Figure 3A, B, S2B)**. Remarkably, in all AT and AB strains, our analysis revealed the presence of cells co-expressing the typical club and goblet cell markers (**Figure 3C**). These Uteroglobin/MUC5AC-positive hybrid cells may represent a transitory state in which one cell type could differentiate into the other, as already described by other groups [25,56]. Furthermore, to assess the ability of *in vitro* expanded cells to develop a native-like regenerated airway epithelium, we set up an air-liquid interface (ALI) culture that better mimics the airway physiological differentiative stimuli [57–59] (**Figure 3D**). In this condition, AT and AB cells were able to regenerate a mature, fully-differentiated airway epithelium composed of the main cell types observed in native tissue (**Figure S1**), namely basal cells, goblet and ciliated cells - responsible for mucociliary clearance – and secretory club cells (**Figure 3E**). Of importance, the presence of properly organized cilia at the apical level demonstrated the correct polarization of the regenerated epithelia while the secreted mucous denoted goblet cells functionality (**Figure 3E**).

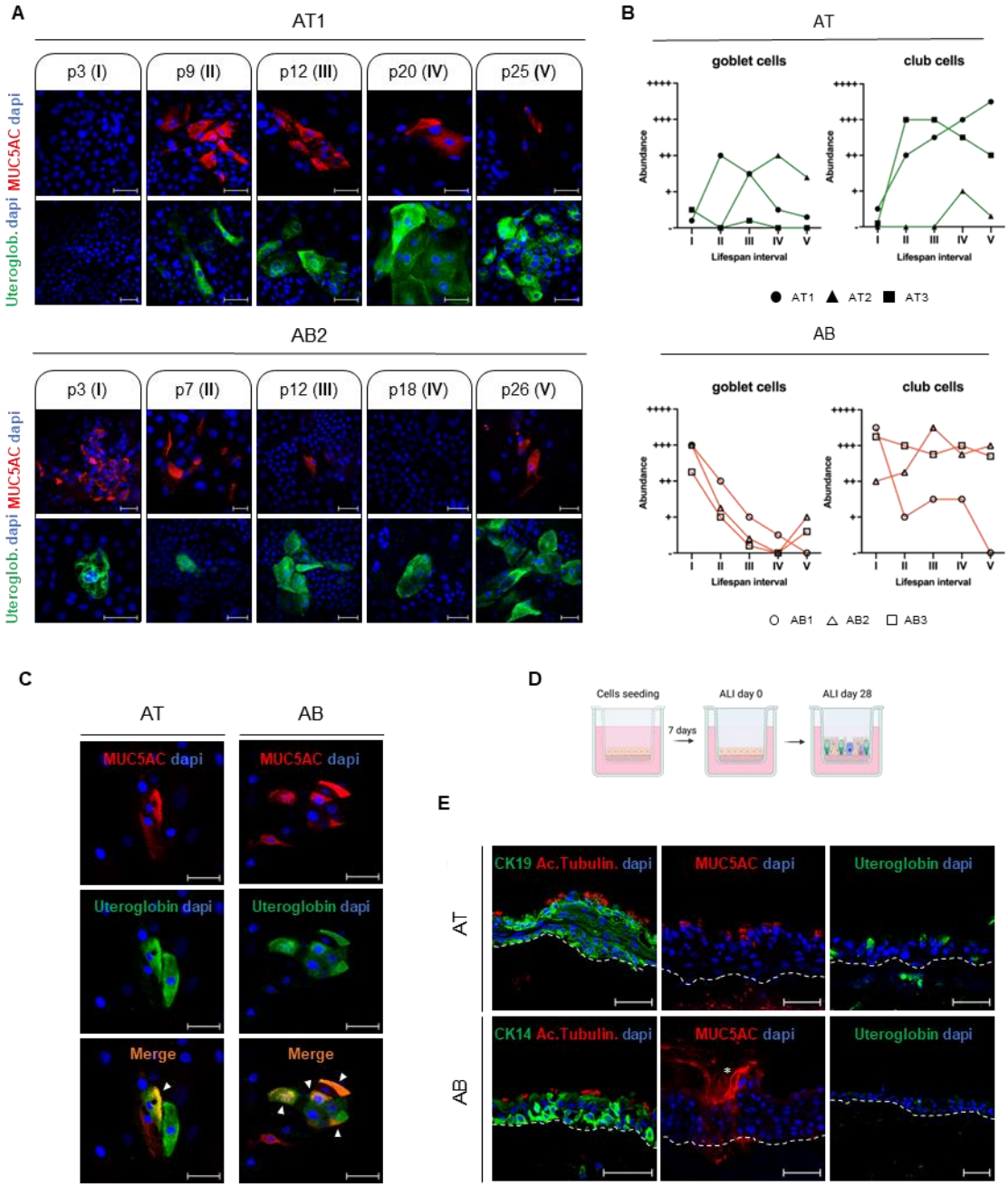

Figure 3. Regenerative and Differentiative Properties of Human Airway Cultured Cells
(A) IF images showing goblet (MUC5AC-positive) and club (Uteroglobin-positive) cells within progressive passages of AT1 (upper panel) and AB2 (lower panel) cultures' lifespan. The same analysis was repeated for n = 3 AT and n = 3 AB primary independent strains. Scale bars, 50 µm.

(B) Graphical representation of the abundance of goblet and club cells in AT (upper panel) and AB (lower panel) cultures' lifespan. Data collected from n = 3 AT and n = 3 AB independent strains indicated with different shapes. Grading definition: -, none; +, low; ++, moderate; +++, high; ++++, very high (see "Star Methods").
(C) IF images of MUC5AC (red) and Uteroglobin (green) staining in AT end AB cultures. The merge highlights the presence of double-positive cells co-expressing MUC5AC and Uteroglobin. White triangles highlight MUC5AC/Uteroglobin-positive cells. These hybrid cells were observed in n = 3 AT and n = 3 AB independent strains. Scale bars, 50 μm.
(D) Cartoon showing air-liquid interface (ALI) culture protocol. From left to right: cells are seeded onto a de-epithelialized human matrix, cultured for 7 days in submerged condition and exposed to ALI for 28 days.
(E) Representative images of the epithelium regenerated by AT (n = 3) and AB (n = 3) independent human strains (n = 9 technical replicates). Dotted line marks the epithelial basal layer. Scale bars, 50 μm.

Epithelial Functional Assays

Once evaluated the efficiency of the cell culture system in expanding human airway epithelial cells and regenerating a fully-differentiated epithelium, we tested its functionality in terms of ability to perform wound healing and act as a physical barrier. The scratch assay experimental setting included a comparison between our clinical-grade culture system (CG) and the commercial Bronchial Epithelial Cell Growth Medium BulletKit™ (BEGM™ from Lonza) as a reference to relate the performance of the two culture systems. Therefore, we produced an *in vitro* wound performing a scratch on tracheal and bronchial epithelia grown in the two culture conditions (see "Star Methods"). Surprisingly, AT and AB epithelia cultivated in CG closed the wound area within 15 hours, while the counterparts grown in BEGM™ did not complete the wound healing process even after 40 hours (**Figure 4A, B, Supplementary video 1**).

The key feature of all epithelial tissues - namely the barrier function - was then assessed by measuring transepithelial electrical resistance (TEER) during the regeneration of AT and AB epithelia in ALI conditions. TEER measurements, performed each 4-6 days, highlighted a constant increase in TEER values throughout the ALI culture, reaching the maximum peak of 421 ± 97 Ω for AT and 361 ± 54 Ω for AB on day 29 of maturation (**Figure 4C**). These results are consistent with the dense network of tight junctions observed in the culture exponential growth phase (**Figure 2**) and point out the regenerated epithelium's ability to function as an efficient barrier. Alongside, the scanning electron microscopy (SEM) analysis confirmed the compactness and well-polarization of AT and AB regenerated epithelia, showing large areas densely covered with cilia and shorter microvilli protruding apically from airway columnar cells (**Figure 4D**). When detached from the support, the ability of clusters of ciliated cells to move and spin within the culture plate suggested the functionality of this peculiar cell population, capable of synchronously beating to move the mucus (**Supplementary video 2**).

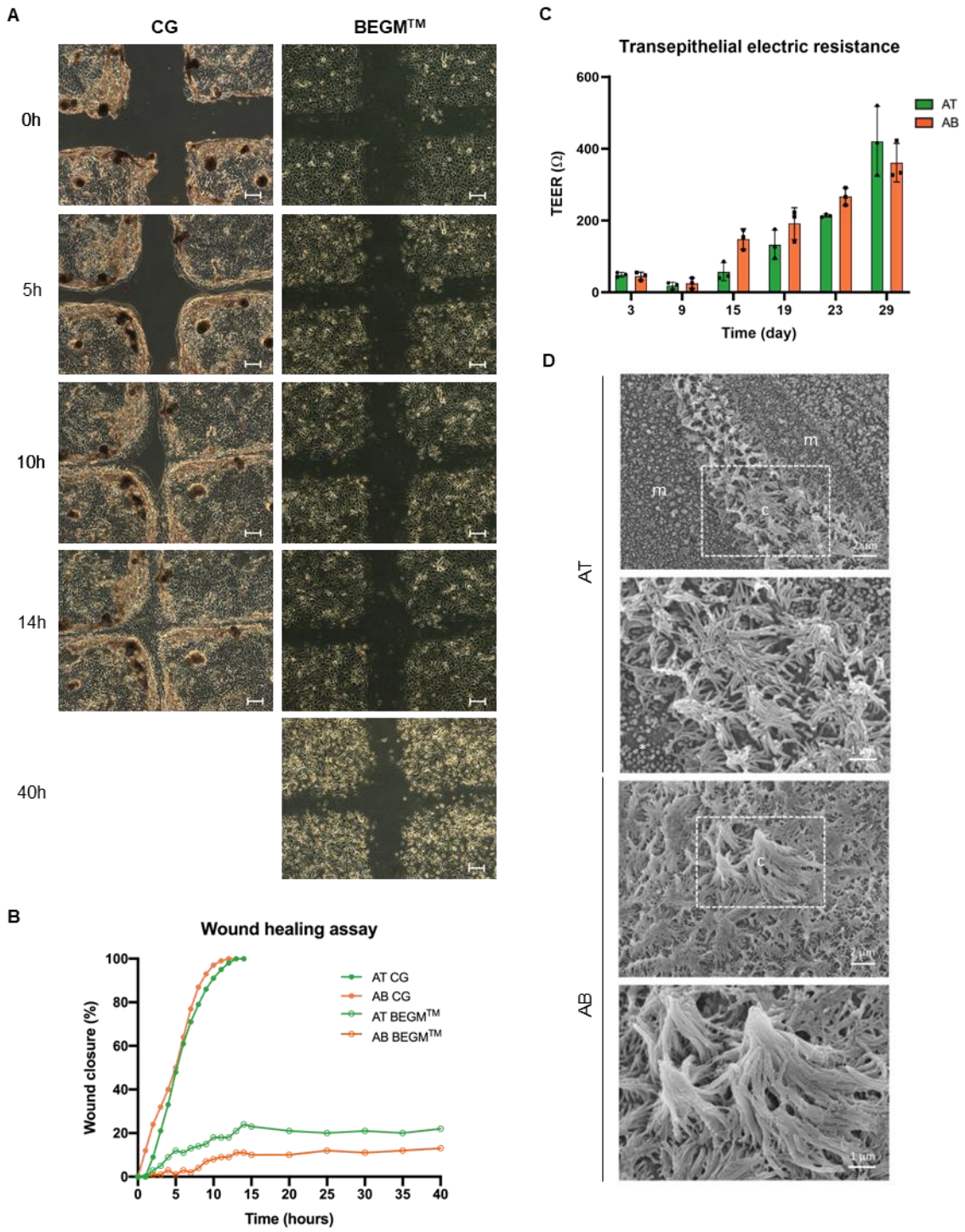

Figure 4. Assays to Evaluate the Functionality of the Regenerated Airway Epithelium

(A) Representative images of airway epithelia grown in CG (left) or BEGM™ (right) culture system at five consecutive time points after the scratch (0h) acquired in live-imaging (Cell Observer®, Zeiss). The assay was conducted on n = 1 AT and n = 1 AB primary cultures from independent donors. Scale bars, 50 µm.

(B) Quantification of the percentage of *in vitro* wound closure in AT and AB epithelial under CG or BEGM™ culture conditions (see "Star Methods"). Wounded area quantified with AxioVision version 4.8.

(C) Graph showing the TEER measurements conducted at six consecutive time points during the AT (green bars) and AB (orange bars) ALI cultures. Average and standard deviation displayed per each time point from technical triplicates of n = 1 AT and n = 1 AB strain. TEER measurements conducted with ERS-2 voltmeter (see "Star Methods").

(D) Representative SEM images of AT and AB regenerated epithelia showing apical cilia (c) and microvilli (m). Dotted square highlighted the area magnified in the inferior image.

Basal Nature of Airway Cultures: Single-cell Clonal Analysis

To understand the mechanisms underlying tracheobronchial culture regeneration, we focused on the clonogenic cell fraction. Specifically, AT and AB cells were seeded at clonal dilution, and all the grown clones were evaluated for the expression of key markers. IF staining revealed that all clones were positive for CK14, suggesting that the regeneration process originates from basal epithelial cells (**Figure 5A, B**). This finding aligns with our previous data on bulk culture, where all the growing colonies exhibited positive staining for CK14 (**Figure 2A, B**). Additionally, the observations made by Kumar and colleagues [60], who reported uniformly stained single airway clones for CK5 and p63 - two widely recognized basal markers - appear consistent with our results (**Figure S2A)**. To investigate the kinetics of differentiation *in vitro*, we explored if, in this early stage of growth (clonal level), the basal cells were already differentiating in club and goblet cells. Uteroglobin-positive club cells were detected within 33% of AT and 72% of AB clones (**Figure 5A, B**), while MUC5AC-positive goblet cells were only detectable in bronchial clones (10%) (**Figure 5A, B**). These insights suggest a precocious ability of basal cells to give rise to specialized cell types, yet with some differences between the two airway compartments. Indeed, the higher abundance of AB clones containing club cells coupled with the absence of AT clones enclosing goblet cells confirmed our previous findings (**Figure 3B**), showing a more rapid commitment of the bronchial tissue towards differentiation lineages.

Basal Cells Heterogeneity

Once the basal epithelial nature of clonogenic cells was confirmed, more accurate analyses were conducted to clarify whether this cell population is homogeneous in its regenerative potential. To this end, single cells from AT and AB subconfluent cultures were seeded at clonal dilution and, after seven days of culture, a part of each clone was plated in a CFE indicator dish for the growth potential evaluation (see "Star Methods") (**Figure 5C**). The ratio between aborted and total colonies revealed the heterogeneity of airway basal cells' clonogenic potential, allowing to classify founder clones into three main categories, according to what was previously described for the epidermis [61] and other epithelial tissues [49,50,62]. These clonal types were characterized by a progressively lower regenerative potential and classified as holoclone (H, which gives rise to 0-5% of aborted colonies), meroclone (M, which gives rise to 5-95% of aborted colonies), and paraclone (P, which gives rise to 95-100% of aborted colonies) (**Figure 5D**). Additionally, to further investigate the wide class of meroclones, they were subdivided into three subgroups, namely early meroclone (EM, 5-20% aborted colonies), intermediated meroclone (IM, 20-60% aborted colonies), and late meroclone (LM, 60-95% aborted colonies) (**Figure 5D**).

Holoclone-forming Cell as the Stem Cell of the Tracheobronchial Epithelium

With the aim of evaluating if, as demonstrated in other human epithelia [39,43,49,63,64], the holoclone-forming cell is the adult stem cell of the tracheobronchial tissue we exposed the progeny of each clone to strong differentiation stimuli to assess the maintenance of the self-renewal ability *in vitro*. After cloning, one-third of each clone was plated in the indicator dish for the clonal classification, while the remaining two-thirds were cultured for 28-30 days, after which the regenerative potential of the clonal progeny was measured through CFE assay (see "Star Methods"). Under this prolonged and extreme differentiative culture condition only stem cells, endowed with self-renewal ability, can abide without a complete exhaustion of the regenerative potential. This assay clearly showed that only the progeny of the clones with less than 6% of aborted colonies retain a significant clonogenic potential after stratification occurring in the prolonged culture period (**Figure 5E, S3A, B**). Therefore, these clones' progeny proved to contain stem cells able to resist this strong differentiation stimulus by self-renewing and dividing into daughter cells still able to regenerate the tissue. Beyond this threshold, all the other types of clones - containing only transient amplifying cells - underwent terminal differentiation reaching the replicative senescence. Accordingly, we considered 6% of aborted colonies as the new threshold value to define H in the human tracheobronchial epithelium (**Figure S3A, B**). The resulting statistical difference among the residual clonogenic ability of H *vs* all the other clonal types was impressive (**Figure 5F**). Indeed, only very few EM showed residual growth potential with a negligible number of grown colonies, which were almost entirely aborted and unable to further proliferate (**Figure 5E, F, S3B)**.

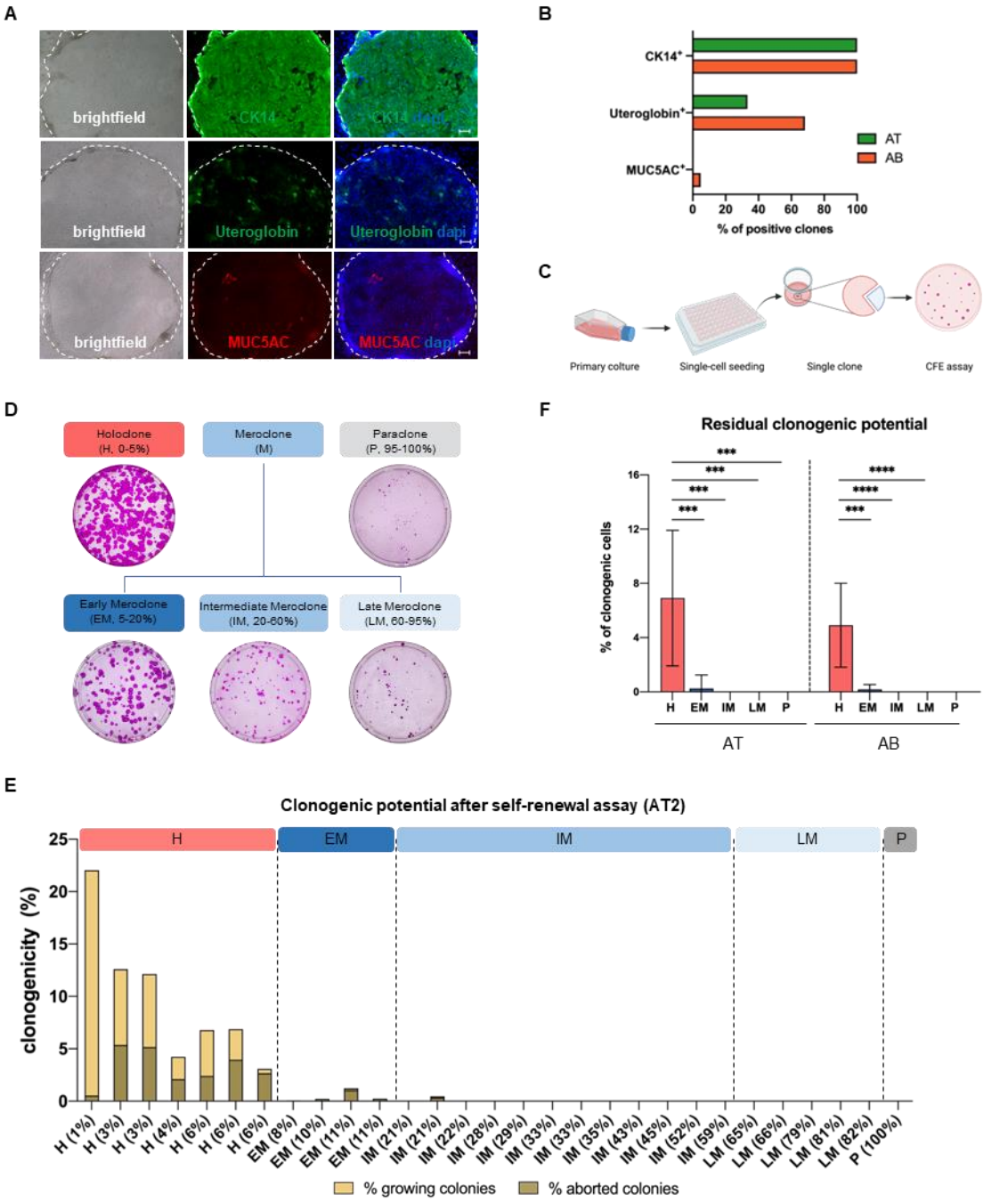

Figure 5. Basal Cell Heterogeneity and Hierarchy

(A) Representative images of airway clones positive for CK14, Uteroglobin and MUC5AC. Brightfield image (left) shows the clone morphology. Clones are indicated with white dotted lines. Scale bars, 50 µm.

(B) Graph showing the percentage of clones positive for CK14, Uteroglobin, and MUC5AC. CK14 staining quantified on n = 63 AT clones and n = 91 AB; Uteroglobin staining quantified on n = 24 AT and n = 29 AB clones; MUC5AC staining quantified on n = 48 AT and n = 29 AB clones.

(C) Schematic representation of clonal analysis procedure. From left to right: sub-confluent primary cultures were trypsinized, serially diluted, and inoculated (1 cell per well) onto 96-multiwell plates coated with irradiated 3T3-J2 cells. After 7 days of cultivation, a part of each clone (one-quarter or one-third) was plated into an indicator dish for the classification of clonal type, see "Star Methods".

(D) Representative images of CFE indicator dishes employed to classify the different types of clones based on the percentage of aborted colonies out of the total number of grown colonies. Analysis conducted on n = 3 independent AT strains (513 total AT clones analyzed in n = 9 clonal analyses) and on n = 2 AB independent strains (167 total AB clones analyzed in n = 4 clonal analyses).

(E) Quantification of the clonogenicity after the self-renewal assay which AT2 clones underwent. Per each clone, the total percentage of grown colonies after 28-30 days of stratification is shown as the sum of the percentage of terminally

differentiated (aborted colonies, light brown) and the percentage of colonies still able to regenerate the tissue (growing colonies, light yellow). AT2 analysed clones: H, n = 7; EM, n = 4; IM, n = 12; LM, n = 5; P, n = 1.
(F) Graphs showing average AT and AB residual clonogenic potential values after stratification of H, EM, IM, LM, and P progeny. The high standard deviation reflects the heterogeneity of H (0-6% of aborted colonies). Analysis conducted on n = 3 AT strains (H, n = 14; EM, n = 14; IM, n = 29; LM, n = 13 and P, n = 20) and n = 1 AB strain (H, n = 15; EM, n = 4; IM, n = 7; and LM, n = 2). Unpaired, biparametric, two-tailed Welch's t test. Values are shown as mean ± SD. ***$p < 0.001$. ****$p < 0.0001$.

Stem Cell Markers Evaluation Within Tracheobronchial Clones

After establishing that the clonal analysis could also be adopted for identifying stem cells within tracheobronchial cultures, we explored more streamlined techniques to prospectively identify and quantify this critical population [40,65]. At first, we measured the clones' area to evaluate if the H's size could univocally distinguish this clonal category from the others. While an increasingly significant difference was observed in AT strains comparing the H's size with EM, IM and P, no differences were detected among AB clones (**Figure 6A**), consistent with previous findings [38,65]. Nevertheless, as clearly visible from the clones' size distribution, the H of AT cultures cannot be univocally identified only based on their size (**Figure 6A**). The same concept also applies to the growth rate in terms of doubling time (**Figure S4 A, B**), excluding these methods to quantify the stem cell content in airway cultures. Afterwards, we investigated if the decreased expression of p63α, BMI1, and SOX2 associated with proliferative senescence (**Figure 2C, D**) was correlated to a differential expression of these TFs in airway clones with various regenerative potentials (**Figure 2C, D**). Indeed, during epithelial serial cultivation, the mass culture composition changes from a population enriched in stem and early progenitor cells (H and EM) in the first passages to a population predominantly composed of old transient amplifying and terminally differentiated cells (LM and P) in the latest passages. This phenomenon is called clonal conversion [66–68]. In WB analysis, p63α, BMI1 and SOX2 expression was found to progressively decrease from H to LM/P, with a notable difference even between H and EM (**Figure 6B, C, S4C, D**). These findings suggest that the expression of these TFs could be exploited, in combination with other biological parameters, to identify and quantify the stem cell population in human airway epithelial cell cultures. However, these markers are not exclusively expressed by stem cells, therefore their mere expression in an airway epithelial culture cannot be used as a univocal marker to discriminate the presence/absence of stem cells within that culture.

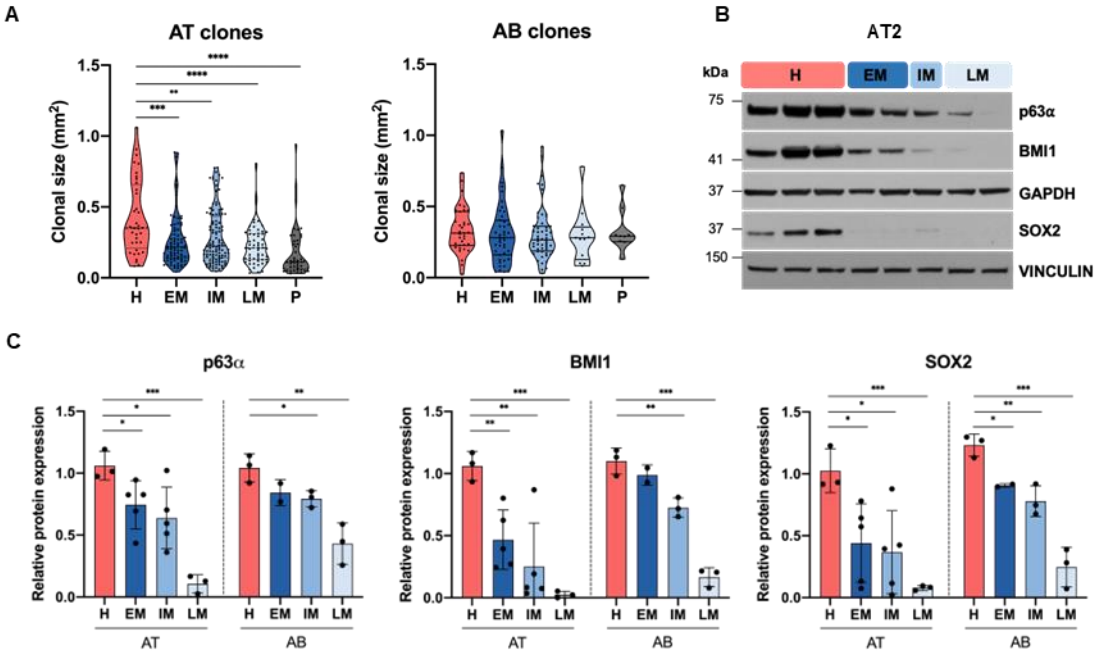

Figure 6. Morphological and Molecular Characterization of Airway Clones

(A) Violin plot showing the size measured in mm^2 of AT (left) and AB (right) different clones. AT analysed clones: H, n = 36; EM, n = 86; IM, n = 112; LM, n = 56; P, n = 45 belonging to n = 3 independent AT strains; AB analysed clones: H, n = 35; EM, n = 44; IM, n = 52; LM, n = 13; P, n = 9 belonging to n = 2 independent AB strains. Dots represent single clones. Median, first and third quartiles are displayed.

(B) WB analysis on total cell extracts from the progeny of AT2 clones (H, n = 3; EM, n = 2; IM, n = 1; LM, n = 2) immunostained with indicated antibodies (image representative of n = 2 analysis conducted on independent clones). Due to their very limited residual proliferative potential, the amount of material collected by AT2 paraclone's progenies was not sufficient to carry out a reliable WB analysis.
(C) From left to right, histograms showing the quantification of the expression levels of p63α, BMI1 (normalized per GAPDH) and SOX2 (normalized per GAPDH in AT and Actin in AB). Average and SD displayed per each clonal category (see "Star Methods"). AT2 analysed clones: H, n = 3; EM, n = 5; IM, n = 5; LM, n = 3. AB1 analysed clones: H, n = 3; EM, n = 2; IM, n = 3; LM, n = 3. Unpaired, biparametric, two-tailed t test *$p < 0.05$.; ** $p < 0.01$; *** $p < 0.001$ and **** $p < 0.0001$.

Differentiative Potential of Human Airway Epithelial Clones

After proving the tracheal and bronchial epithelial basal cells heterogeneity and assessing their hierarchy, we wondered if the ability to give rise to the multiple differentiated airway lineages specifically correlates with the stemness or if it is maintained during commitment. Consequently, we performed two complementary sets of experiments, where each clone was cultured in standard submerged conditions or in ALI to evaluate its differentiative potential (**Figure 7A**). The submerged cultures allowed the detection of club and goblet cells in the progeny of AT and AB H, EM, IM, and LM, while in P progeny only a few scattered goblet cells were observed (**Figure 7A, left panel**). Worth of note, as previously observed in the cultures' lifespan (**Figure 3C**), Uteroglobin/MUC5AC-double positive cells were also found in submerged H and M' progenies (**Figure 7B**). In parallel, ALI cultures displayed ciliated cells in the apical side of the epithelia regenerated from H, EM, IM and LM, completing the analysis of the clones' differentiation potential (**Figure 7A, right panel**). These findings formally proved that a single airway epithelial basal cell has the potential to regenerate a fully differentiated and specialized tracheobronchial epithelium. This multipotency, contrary to self-renewal, is not restricted to the stem cells (holoclone-forming cells) but is also shared with their progenitors (meroclone-forming cells). Instead, the paraclone-forming cells, the ultimate status of proliferating basal cells, showed a limited differentiation ability, as proven by the presence of goblet but not club cells in their progeny (**Figure 7A, left panel**). The heavy differentiation stimuli imposed by 30 days of ALI culture revealed H as able to maintain their fully differentiative potential, whereas M's progeny proceeded toward a terminal differentiation process characterized by the absence of club cells within most of the regenerated epithelia, although they were visible in their submerged counterpart. Finally, P were totally unable to regenerate an epithelium (**Figure 7A, right panel**). Overall, these findings remarked the H-forming cells as the most powerful and resilient cells, able to withstand the ALI terminal differentiation stimuli and guarantee complex tracheobronchial cellular heterogeneity.

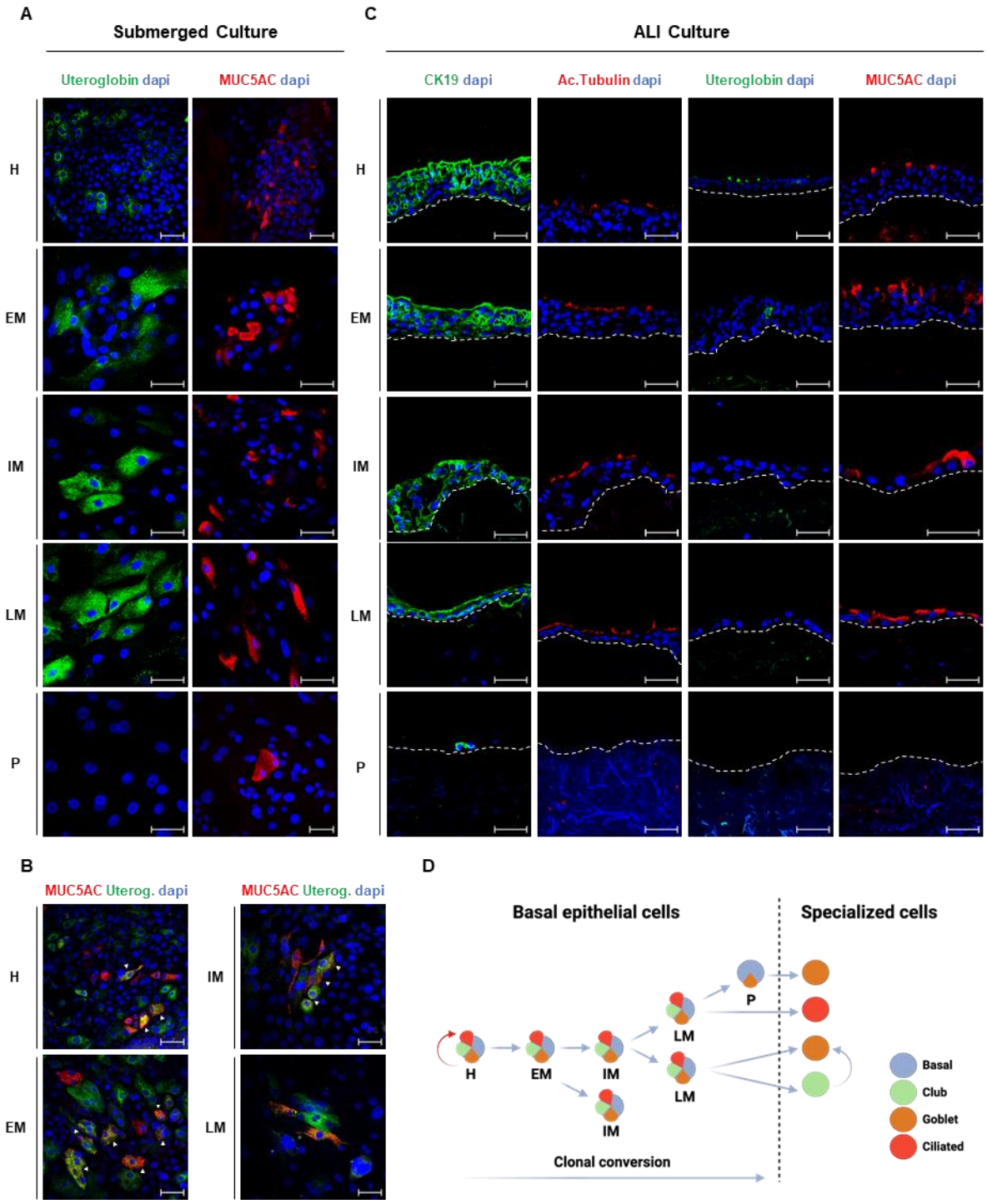

Figure 7. Clones Differentiative Potential

(A) Representative IF images of the different types of AT clones' progeny cultured in standard submerged condition. Analysis conducted on n = 3 AT (H, n = 11; EM, n =10; IM, n = 27; LM, n = 13; P, n = 4) and n = 1 AB strains (H, n = 7; EM, n =6; IM, n =4; LM, n = 4; P, n = 1). Dotted line marks the epithelial basal layer.

(B) Double IF staining of AT and AB epithelial cells revealing co-expression of MUC5AC (red) and Uteroglobin (green) in the progeny of airway H, EM, IM and LM. White triangles highlight MUC5AC/Uteroglobin-positive cells.

(C) Representative IF images of the different types of AT clones' progeny cultured in ALI conditions. Analysis conducted on n = 3 AT (H, n = 9; EM, n = 15; IM, n = 12; LM, n = 10; P, n = 12) and n = 1 AB strains (H, n = 2; EM, n = 1). Dotted line marks the epithelial basal layer.

(D) Cartoon showing a model of *in vitro* human airway epithelium renewal and clones' differentiative potential. H, EM, IM and LM basal clonal display a multipotency in differentiating in club, goblet and ciliated cells while paraclone can only give rise to goblet cells. Among the differentiated cell types, club cells can differentiate in goblet cells.

DISCUSSION

The clinical outcomes of TE approaches aimed at treating wide tracheal and bronchial defects have highlighted the inability to regenerate large areas of a fully-differentiated, functional and self-renewing airway epithelium in the bioengineered graft [8,21–23]. One of the main challenges has been the limited lifespan of primary airway epithelial cells, which showed efficient division for only a limited number of passages before becoming senescent and losing their differentiation potential [23,26–32]. Herein, we demonstrated that, under appropriate culture conditions, human airway epithelial cells exhibit huge proliferative potential, undergoing numerous consecutive sub-culturing passages and cell duplications that extensively fulfil the requirements for transplantation. Importantly, the culture system we employed has been already clinically validated for the regeneration of other human epithelial tissues [35–37,42,43,63,64,69,70]. In this work, all AT and AB epithelial cell cultures physiologically reached replicative senescence with a gradual decline in clonogenicity and p63 expression. The absence of immortalization events pointed out the safety of this expansion procedure, making it more suitable for clinical applications compared to other approaches. Indeed, besides immortalization procedures [26–28,71,72], that inherently cannot be applied in a clinical setting [73,74], methods based on the pharmacological inhibition of Rho kinase (ROCK) [33,75–78] or dual SMAD inhibition [79,80] are associated with some safety constraints. In fact, although these methods might prove useful for modelling the airway epithelium *in vitro* [79], the inhibition of these pathways significantly alters epithelial physiology modifying stem cell proliferation, differentiation, and cell cycle regulation [81–84]. These alterations compromise airway cell terminal differentiation and lead to the transient immortalization of the culture, forcing it toward a stem cell-like phenotype [32]. In addition to proliferative potential preservation, the maintenance of differentiative capacity, equally crucial, was not thoroughly reported in most unsuccessful clinical TE attempts [15,16]. Here, we demonstrated the suitability of clinical grade expansion conditions in preserving cell heterogeneity and regenerating a fully differentiated airway epithelium able to act as an efficient barrier against environmental insults and infections. Further studies will verify whether this epithelium, composed of basal, club, goblet and ciliated cells also comprises rarer airway cell types. Notably, the ability to promptly close a wound, a key feature in TE approaches, was assured with our system but not using a defined commercially available cell culture medium.

As the second part of this study, we focused on airway epithelial stem cell identification and characterization. Indeed, the regeneration of tissues subjected to a self-renewal process is strictly dependent on the presence of functional tissue-specific stem cells [64,85–89]. In addition, more than three decades of clinical application in the engineering of highly renewing human epithelial tissues have emphasized that the preservation of the stem cells in culture is the key feature determining the success or the failure of the treatment [35,36,38,42,90]. Our data revealed that the entire clonogenic compartment is made of basal cells, strengthening the notion that human tracheal and bronchial epithelia have a basal origin [46,60,91,92].

Remarkably, we formally proved that airway clonogenic cells are heterogenous in their regenerative capacity and, as previously demonstrated for other human epithelia [49,50,61,62], can give rise to holoclones, meroclones, and paraclones. Of utmost importance, we highlighted that tracheal and bronchial holoclone-forming cells possess peculiar hallmarks of epithelial stem cells, therefore identifiable as the stem cells of the airway tissue. Indeed, coherently with what was observed in other epithelia [36,43], human airway holoclone-forming cells but not meroclones and paraclones are able to self-renew and withstand strong differentiation stimuli. Alongside, meroclones and paraclones, being transient progenitors, progressively lose their proliferative potential and thus contribute to tissue regeneration for a limited amount of time. Notably, despite all holoclones showed self-renewal ability, the variable clonogenic potential after stratification contributes to the ongoing debate regarding whether all holoclone-forming cells are identical or if a hierarchical relationship exists among them [36]. What is certain so far is that not only holoclones must be present but an adequate quantity of them is required to achieve long-term successful therapies [38,42]. Our results established that the gold standard method adopted for stem cell quantification in other epithelia, namely the clonal analysis, can be also employed to assess the preservation of airway holoclones upon expansion and throughout the most critical steps of the TE procedure. However, albeit effective, this control is extremely cumbersome and time-consuming [38,65], therefore the evaluation of more direct methods to prospectively identify and quantify stem cells within epithelial culture appears of prime importance [65,93]. Our initial attempts to utilize clone size or growth rates as biological parameters to distinguish holoclones from other clonal categories proved unsuccessful, in line with what was reported for other epithelial tissues [43,50,61,65,94]. Instead, the analysis of transcriptional factors p63α, BMI1, and SOX2 provided more substantial outcomes. In fact, consistent with what was observed during airway epithelial cell lifespans, these TFs exhibited differential expression among holoclones, meroclones, and paraclones,

strengthening their potential correlation with stemness. Indeed, p63 is indispensable for preserving the stem cells' proliferative potential in adult stratified epithelia [67,95–97], including the airway epithelium, where p63-deficient mice completely lacked airway basal cells [54]. Likewise, BMI1 plays a crucial role in maintaining self-renewal in a variety of adult stem cells including hematopoietic [98], nervous [99], and bronchioalveolar stem cells (BASCs) [52]. Specifically, BASCs lacking BMI1 display reduced proliferative capacity and clonogenicity, with colonies of smaller size compared to their wild-type counterpart [52]. Ultimately, SOX2 is fundamental in embryonic stem cells self-renewal and pluripotency [53,55] but also in lung development [100], where it plays a key role in airway epithelial proliferation and lineage specification [101,102]. Notably, SOX2 overexpression in respiratory epithelium leads to an increased number of p63-positive cells, suggesting its implication in the maintenance of basal stem cells [100]. Moreover, our findings describing p63 and BMI1 differential expression in airway clones align with the previously reported patterns in the epidermal, corneal, oral mucosa and urethral clones [49,51,67,93]. Specifically, limbal stem cells can be prospectively identified by p63 abundance through a bi-parametric analysis correlating its expression level with cellular dimension [40]. The robust association between the number of p63-bright holoclones quantified in limbal cultures and the clinical success confirmed p63 as a potency marker [38,42], leading to the first tissue engineering stem-cell-based ATMP (Holoclar®) approved by European Medicinal Agency (Pellegrini et al., 2018) [34]. Drawing insight from these principles, the differential expression of the aforementioned TFs within airway clones can be further explored to assess the feasibility of prospectively quantifying the percentage of holoclone-forming cells within an airway culture destined for cell therapy and TE approaches. Indeed, such an inquiry has the potential to advance airway TE towards a more standardized, safe, and effective therapy. Nevertheless, the presence of p63, BMI1, and SOX2 not being restricted solely to holoclones indicates that their expression alone cannot serve as an absolute indicator for identifying the presence of stem cells within the culture. Consequently, to gain meaningful insights, the differential level of expression can be quantified and correlated with other critical biological attributes. Finally, this study unraveled the role of stem and progenitor cells in regenerating the tissue and preserving airway epithelial heterogeneity (**Figure 7D**). Indeed, we showed that a single airway basal cell can regenerate a fully specialized airway epithelium composed of all primary cell types that characterize the native tissue. These findings complement the observations made by Kumar and colleagues [60], extending the differentiation potential of a single tracheal epithelial basal cell to encompass club cells, in addition to ciliated and goblet cells. Moreover, during clonal conversion, this multipotency is maintained up to the late meroclones (**Figure 7D**). Consequently, not only stem cells but also progenitors are responsible for replenishing differentiated cell lineages during airway epithelium physiological turnover or wound healing. A similar mechanism was described for conjunctival epithelium, where goblet cells originate from both stem and progenitor cells [50]. Besides, the fact that P were unable to give rise to club cells could be explained by the hypothesis that the paraclone-forming cell, being the most differentiated status of epithelial basal cell, could not generate cells endowed with progenitor properties such as club cells [103–106]. Moreover, the earlier appearance of club cells compared to goblet cells within the whole-stained airway clones, coupled with the lack of club cells within the M airlifted cultures and the presence of MUC5AC/Uteroglobin-positive cells - also reported by other groups [25,56,79,107,108] - further support the progenitor role of club cells in airway epithelium. Indeed, it seems plausible that club cells can convert into other specialized cell types, including goblet cells [107,109,110]. This assumption aligns with findings from animal models involving injury and lineage-tracing experiments [25,103,111], as well as with hypotheses derived from single-cell RNA sequencing analysis in humans [56]. Additional research is necessary to confirm the potential for club and goblet cells to directly differentiate into ciliated cells as reported by relevant papers [56,112].

Overall, our data demonstrated that, under an appropriate culture system, autologous human airway epithelial cells are a suitable cell source for TE approaches. Rather, inadequate culture conditions can speed up airway clonal conversion, causing premature exhaustion of the stem cell population, as also demonstrated for epidermal keratinocytes [68]. In such scenarios, the culture could not result in the stable regeneration of the airway epithelium once transplanted, ultimately triggering the failure of the TE approach with severe consequences for patients' health. Therefore, we suggest in-process controls to be performed throughout the manufacturing procedure to ensure the airway epithelium quality within the bioengineered graft. These quality controls encompassed (*i*) the airway biopsy collection and cell extraction methods, which both have a significant impact on the cell culture performance and the overall reproducibility of the results, (*ii*) the characterization of the airway cultured cells to comply with safety and identity requirements, and (*iii*) the assessment of an adequate number of stem cells to guarantee the long-term regeneration of the graft. This last prerequisite should be verified through a rigorous clonal analysis until new, more straightforward methods are refined.

We strongly believe that the insights gained in tissue-specific biology and epithelial regeneration under *in vitro* expansion can tackle critical hurdles in airway TE, thereby fostering safe and effective translational research.

ACKNOWLEDGMENTS
We would like to thank Anna Ribbene and Sonia Carulli for their help with cell culture. This study was supported by Progetto di ricerca di rilevante interesse nazionale (PRIN) prot. 2022CMNWCZ and funded by BIOtrachea (EU-FP7 project reference: 308439), the Award "Lombardia è Ricerca 2018", by "Louis Jeantet Award 2020", and by FAR 2020 DIP - Fondo di Ateneo per la Ricerca per il finanziamento di progetti di ricerca dipartimentali.

AUTHOR CONTRIBUTIONS
Conceptualization: D.A., V.G.G., G.P; formal analysis: V.G.G., D.A., GG.; investigation: D.A., V.G.G., G.G., C.C., A.M., F.L., F.B.; human samples collection: F.L.C, J.E.; writing-original draft preparation: D.A., V.G.G., G.G.; writing-review and editing: D.A., V.G.G., G.G., C.C, A.M., F.L., F.B., D.Q., J.E., F.L.C., G.P.; supervision: G.P.; funding acquisition: G.P. All authors have read and agreed to the published version of the manuscript.

DECLARATION OF INTERESTS
The authors declare no competing interests.

STAR METHODS

1. RESOURCE AVAILABILITY

Lead contact
Further information and requests for resources and reagents should be directed to and will be fulfilled by the Lead Contacts, Davide Adamo (davide.adamo@unimore.it).

Materials Availability
This study did not generate new unique reagents. The Mouse 3T3-J2 cells used as a feeder-layer (FL) for the growth of primary human AT and AB epithelial cells were received as a gift from Prof. Howard Green, Harvard Medical School (Boston, MA, USA).

Data and Code Availability
This paper does not report original codes. Any additional information required to reanalyze the data reported in this paper is available from the lead contact upon request.

2. EXPERIMENTAL MODEL AND SUBJECT DETAILS

Human samples
Human tracheal and bronchial samples were collected from living donors as by-products from surgical waste (tracheal resections for laryngeal-tracheal stenosis or pulmonary lobectomy). All donors, n=5 males and n=5 females aged between 38 and 76 years, agreed to the use of their biological material for the present study and signed the informed consent. In compliance with Italian regulations, ethical committee approval was obtained from all involved centres "Arcispedale S. Maria Nuova di Reggio Emilia", IRCCS, Reggio Emilia, Italy, ("Comitato Etico Area Vasta Emilia Nord", Protocol N. 2019/0014725), and the "Fondazione Policlinico Universitario A. Gemelli", IRCCS, Rome, Italy ("Comitato Etico Territoriale Lazio Area 3" N. 0008968/21). Exclusion criteria implied patients suffering from neoplastic diseases or infections like aspergillosis, nocardiosis, tuberculosis or SARS-CoV-2. Human skin samples were obtained from "Azienda Ospedaliero-Universitaria di Modena", IRCSS, Modena, Italy" from healthy living donors as by-product of surgical waste (abdominoplasty or mammoplasty) upon informed consent and compliance with Italian regulations (Comitato Etico dell'Area Vasta Emilia Nord, number 178/09). All specimens were obtained in accordance with the tenets of the Declaration of Helsinki and were anonymized by the PI in the operating room for privacy reasons.

Cell lines and primary cell culture

After collection in the surgery room, tracheal and bronchial biopsies were shipped from the clinical centres to the "Centre for Regenerative Medicine of Modena and Reggio-Emilia, Modena, Italy" through a clinically validated, temperature-controlled transport packaging. Subsequently to the transport within a clinical-grade culture medium and no more than 36 hours after sample collection, biopsies were minced and dissociated with 0.05% trypsin (Thermo Fisher Scientific, Waltham, Massachusetts, USA) and 0.01% 2,2′,2″,2‴-(Ethane-1,2-diyldinitrilo) tetra-acetic acid (EDTA) at 37°C for 4-12 cycles of 30 minutes (min). Every 30 min, epithelial cells were collected, plated ($2.5–3 \times 10^4/cm^2$) on GMP-certified lethally irradiated 3T3-J2 cells ($2.4 \times 10^4/cm^2$), and grown at 37 °C, 5% CO_2 in 95% humidified atmosphere in a medium named KNO composed of Dulbecco's modified Eagle's (DMEM) and Ham's F12 media (2:1 mixture, (EuroClone, Milan, Italy), 10% fetal bovine serum (FBS, Thermo Fisher Scientific), 50 lU/ml penicillin–streptomycin (EuroClone, Milan, Italy), 4mM glutamine (EuroClone, Milan, Italy), 0.18 mM adenine (Merck, Darmstadt, Germany), 5 mg/ml insulin (Eli Lilly and Company, Indianapolis, Indiana, USA), 0.1 nM cholera toxin (List Biological, California, USA), 0.4 mg/ml hydrocortisone (Avantor, Pennsylvania, USA), 2 nM triiodothyronine (Peptido Gmbh). At the first feeding time, three days after plating, 10 ng/ml epidermal growth factor (EGF, Austral Biologicals, California, USA) was added at KNO medium (KC medium). Primary cultures were fed every other day with KC medium. When airway cultures reached subconfluence, the epithelial cells were dissociated at 37°C for 15 min in trypsin and either frozen at -196°C in freezing medium composed of 10% glycerol (Johnson & Johnson, New Brunswick, New Jersey, USA) in KNO medium, or serially propagated at a density of $6x10^6$ cells/cm^2 until replicative senescence [50]. All the reagents used for the cell extraction and culture were extensively selected and screened for contaminants and cytotoxic effects absence.

Mouse 3T3-J2 cells, used as FL for human epithelial cells, were cultivated in DMEM supplemented with 10% gamma-irradiated donor adult bovine serum, penicillin–streptomycin (50 IU/ml) and glutamine (4 mM) and detached with 0.25% Trypsin-EDTA 1X (Thermo Fisher Scientific, Waltham, Massachusetts, USA).

3. METHOD DETAILS

Colony-forming efficiency assay, population doublings and growth rate (doubling time)

Colony-forming efficiency was calculated after cell extraction from human biopsy and at each serial passage serial passage of tracheobronchial lifespans from the indicator dish stained with rhodamine B (Sigma-Aldrich, St. Louis, Missouri, USA) after 12 days of cultivation. Briefly, a small aliquot of cells - ranging from 200 to 2000 - was plated onto indicator culture dishes previously seeded with 3T3-J2 FL and cultured following the abovementioned protocol. Under examination with a dissecting microscope, colonies were scored as progressively growing or aborted, as previously described [50,61]. The percentage of clonogenic cells corresponds to the number of colonies on the total amount of plated cells, whereas the percentage of abortive colonies was calculated as the number of abortive colonies on the total number of colonies. The following formula was used to score the number of cell doublings: $x = 3.322 \ln(N/No)$, where N is the total number of epithelial cells collected at each passage and No is the number of clonogenic cells plated. Doubling time was calculated using the following formula (number of hours to reach subconfluence/number of cell doublings performed).

Clonal analysis

For the clonal analysis, subconfluent airway cultures were trypsinized and, after limiting dilution, single cells were inoculated into 96-multiwell plates (1 cells per well) coated with a FL of 3T3-J2 cells. After seven days of culture, wells containing single clones were selected under an inverted microscope and each clone was photographed and then dissociated with trypsin digestion to obtain single cells suspension. Afterwards, each cell suspension was divided into three or four parts. Typically, one-third/one-quarter of the clone was plated into an indicator dish for CFE analysis, while the other two-third/three quarter were used in various experiments to characterise each clone's regenerative potential. CFE assay allowed the clonal classification according to the number of aborted colonies. Briefly, clones that generated between 0-6% of aborted colonies were classified as holoclones (H), clones that generated between 6-95% of aborted colonies were classified as a meroclones (M), while clones that generated more than 95% of colonies were classified as paraclones (P). Among meroclones, a further classification distinguished them in early meroclones (EM, 6-20% of aborted colonies), intermediate meroclones (IM, 20-60% of aborted colonies) and late meroclones (LM, 60-95% of

aborted colonies). Clone size has been calculated using ×10 objective and ZEN plug-in AxioVision SE64 software (Rel. 4.9.1, Zeiss, Oberkochen, Germany).

Un-clustered analysis of airway clonogenic cells

Subconfluent airway epithelial cultures were enzymatically detached and, after limiting dilution, single cells were inoculated into 96-multiwell plates containing a FL of 3T3-J2 cells. On the 7th day of culture, single AT and AB clones were fixed with 3% paraformaldehyde in 1x PBS (10 min at RT) or cold methanol (10 min at -20°C) and immunostained as described in the section "Immunofluorescence staining". Images were acquired through Cell Observer Z.1 Microscope (Zeiss) and ZEN plug-in AxioVision software (Rel. 4.8, Zeiss, Oberkochen, Germany).

***In vitro* self-renewal assay**

To evaluate the self-renewal potential of the different clonal category under stressful conditions, AT and AB clones grown as described in "clonal analysis" section were detached and concomitantly seeded into an indicator dish for clonal type classification (one-third of the clone) and cultured in a well of a 24-multiwell plate with KC medium for additional 28/30 days in presence of FL (two-thirds of the clone). During this prolonged culture period, the cell culture medium (KC) was first changed on day three and then daily until 28/30th day of culture. Subsequently, the progeny of each clone was detached and CFE assay was performed. Specifically, we plated 5,000-10,000 cells for H (to allow a precise colony count), while for the other clonal types (M and P), we plated all the detached cells in indicator dishes to provide an overall assessment of residual clonogenicity.

Air-liquid interface culture

For the air-liquid interface culture, tracheal and bronchial epithelial cells derived from subconfluent cultures previously expanded for up to 5 passages were seeded ($2.4 \times 10^4/cm^2$) onto a human- de-epithelialized derma (used as a biological scaffold) coated with FL of lethally irradiated 3T3-J2 cells and located within Millicell® culture plate inserts (Merck Millipore, Burlington, MA, USA). Human AT and AB epithelial cells were cultured onto this matrix submerged by KC culture medium for seven days, after which the KC medium was removed from the apical chamber of Millicell® culture plate inserts to start the air-liquid interface culture. The culture medium was changed every other day until day 28-30. At the end of this period, airlifted cultures were embedded in optimal cutting temperature compound (OCT, Bio-Optica) compound and stored at -80°C until usage. The same protocol has been applied for the airlifted culture of the clonal progenies with the only exception being the seeding density. Indeed, for that experiment three-quarter of each clone was used to set up airlift culture.

De-epithelialization of human dermis

To de-epithelialize human dermis, human skin biopsies derived from abdominoplasty or mammoplasty were subjected to thermal shock. Specifically, specimens were submerged in preheated 1x PBS at a temperature of 60°C for 30 seconds and immediately transferred in a container with 1x PBS at 4°C for one minute. Following this treatment, the epidermis was carefully separated from the dermis using sterile forceps, being cautious to preserve the integrity of the dermal tissue.

Immunofluorescence staining

For immunofluorescence analysis, tracheal and bronchial human specimens and the airlifted cultures on human de-epithelialized derma were embedded in OCT (Bio-Optica) and stored at -80°C. Subsequently, 8-20 µm-thick sections were cut with a cryostat and mounted onto glass slides. These sections, as well as airway epithelial cultures grown onto glass slide coverslip (15.000 cells/ well of a 24-multiwell plate) and single clones grown into the 96-multiwell plates were fixed with 3% paraformaldehyde (10 min at RT) or cold methanol (10 min at -20°C). Then, samples were carefully washed with 1x PBS, permeabilised with 0.5-1% Triton X100 in 1x PBS (10min at RT) and subsequently blocked with blocking solution (BSA 2% in 1x PBS) for 30 min at 37°C or 1h at RT. The samples were first incubated for 30min at 37°C with the primary antibody and later with the appropriate secondary antibody (typically Alexa Fluor conjugates, Thermo Fisher Scientific**,** **Key resource table**) for 30min at 37°C, both diluted in blocking solution. The following primary antibodies were used: Rabbit polyclonal anti-KERATIN 5 (1:1000, Biolegend), rabbit polyclonal anti- KERATIN 14 (1:1000, Biolegend), mouse monoclonal anti- KERATIN 18 (1:100, Abcam), rabbit monoclonal anti-

KERATIN 19 (1:2000, Abcam), mouse monoclonal anti-Involucrin (1:100, Leica Microsystems), mouse monoclonal anti-Acetylated Tubulin (1:100, Sigma), mouse monoclonal anti-mucin (1:20, Progen), rat monoclonal anti-Uteroglobin (1:20, R&D System), rabbit polyclonal anti-ZO-1 (1:100, Thermo Fisher Scientific), rabbit polyclonal anti-Ki-67 (1:100, Abcam), rabbit polyclonal anti-p63-alpha (1:5000, custom), mouse monoclonal anti-14-3-3-Sigma (1:200, Abcam). Cell nuclei were stained with 4',6 diamidino-2-phenylindole (DAPI) for 5 min at RT and coverslips were mounted with Fluorescent Mounting Medium (Dako, Agilent Technologies, Santa Clara, CA, USA). The images of the *in vivo* sections, airlifted cultures sections, and airway epithelial cultures grown onto glass slide coverslip were acquired with a laser-scanning confocal microscope (LSM 900, Zeiss, Oberkochen, Germany) and ZEN 2 software (Rel. 3.3, Zeiss, Oberkochen, Germany). A Zeiss EC PlanNeofluar 40x/1.3 oil immersion objective was used to visualize fluorescent signals. Instead, the images of single clones grown in 96-multiwell plates were acquired through Z1 Motorized Inverted Fluorescence Microscope (Zeiss Axio Observer Z1, Zeiss, Oberkochen, Germany). Per each single clone, the staining for the analysed marker was annotated as positive or negative. Then, the ratio between the number of positive clones and the total analysed clones was calculated.

Airway specialized cell abundance in lifespan serial passages

To determine the abundance of goblet and club cells within serial passages of AT and AB cultures, one entire coverslip from each analysed passage of the cultures was stained for MUC5AC and Uteroglobin (**Key resource table**) and thoroughly screened (from top to bottom) for the presence of these cells. Due to varying expression levels of the aforementioned proteins and a natural stratification of the epithelial colonies, precise quantification of the two cell populations was unattainable. Instead, we assigned a score to each analyzed culture based on the abundance of positive cells. Grading definition: -, no positive cells were present (none); +, less than 10 positive cells present (low); ++, positive cells present in approximately 30% of colonies (moderate); +++, positive cells present in approximately 60% of colonies (high); ++++, positive cells present in approximately 90% of colonies (very high). For each lifespans interval (I-V), multiple cultures on glass slide coverslips have been analysed. Therefore, the grading for each interval was represented as the mean value of these analyses.

Western blotting

For the WB analysis conducted on the serial passages of AT and AB culture lifespans, proteins were extracted from dry pellets using RIPA buffer (Sigma-Aldrich, St. Louis, Missouri, USA, cat#R0278) supplemented with phosphatase and protease inhibitor cocktails (Thermo Fisher Scientific, Waltham, MA, USA, cat#78420, cat#72426) at 0–4°C. The Bradford assay (Bio-Rad, Hercules, CA, USA, cat#500-0006) and the spectrophotometer reading were used to quantify the total protein amount. Equal protein amounts were electrophoresed on NuPage 4-12% Bis-Tris Protein gels (Thermo Fisher Scientific, St. Louis, Missouri, USA, cat#NP0322) and transferred at 100 V and 4 °C for 2 hours onto nitrocellulose membrane (Merck-Millipore, Burlington, MA, USA, cat#1620115). Membranes were treated with blocking solution 5% (w/v) non-fat milk (Bio-Rad, Hercules, CA, USA, cat#1706404) in 0.01% (v/v) Tween-20 (Sigma-Aldrich, St. Louis, Missouri, USA, cat#P1379) in 1x PBS. Protein bands immunoreactions were performed with different primary antibodies (**Key resource table**) diluted in the blocking solution, added overnight at 4 °C to the membranes.
The following primary antibodies were used: rabbit polyclonal anti-p63-alpha (1:5000, customized), rabbit monoclonal anti-BMI1 (1:500, Cell Signalling Technology), rabbit monoclonal anti-SOX2 (1:200, Cell Signalling Technology), mouse monoclonal anti-GAPDH (1:10.000, Abcam), mouse monoclonal anti-Vinculin (1:10.000, Sigma-Aldrich), rabbit polyclonal anti-KERATIN 14 (1:40.000, Biolegend), mouse monoclonal anti-Involucrin (1:10.000, Leica Microsystems), mouse monoclonal anti-Actin (1:5000, Abcam). The corresponding HRP-conjugated secondary antibodies (**Key resource table**) were diluted in the blocking solution and incubated for 1 hour at RT after three washings with 1x PBS. Proteins signals were developed using a chemiluminescent labelling reagent (Supersignal West Pico Chemiluminescent Substrate, Thermo Scientific, cat#34580) and acquired with ChemiDocTM (Bio-Rad, Hercules, CA, USA) and Image Lab software (Bio-Rad, Hercules, CA, USA), while bands quantification was performed with Image J software. Gray background on the images was homogeneously added for graphical purpose. For the WB analysis on AT and AB lifespan, each lifespan was subdivided into five consecutive temporal intervals (I-V) to compare markers' expression levels of the different strains (AT n=3 and AB n =3) in the same airway district. In case of multiple pellets analysed within the same interval, the mean expression value has been considered. Finally, the average and SD of n = 3 AT and n = 3 AB was plotted per each time interval, and the expression level of

each independent strain was indicated with different shapes. For the WB analysis on clonal progeny, the expression values of H, EM, IM, LM and P of both AT and AB clones have been shown for each strain as the mean of the different clones analysed, indicated with dots.

Scanning electron microscopy (SEM)
AT and AB airlifted cultures were fixed in 2.5% (v/v) glutaraldehyde in 0.1M sodium cacodylate for 1 hour at 4°C, washed with 0.1M sodium cacodylate and postfixed in 1% (w/v) OsO_4 (Electron Microscopy Sciences, Hatfield, PA, USA) for 1 hour at room temperature. Samples were dehydrated in an ascending series of ethanol and critical point dried through liquid carbon dioxide. Specimens were mounted on aluminium stubs and coated with a gold sputter. Finally, the samples were observed under a NOVA NanoSEM 450 (FEI company-Thermo Fisher, Hillsboro, OR, USA) and images were acquired in high-vacuum mode with TLD detector operated at 8 kV.

Wound healing assay
To perform the wound healing assay, human AT and AB epithelial cells were plated into rectangular cell culture plates (from Cell Comb Scratch Assay, Merck-Millipore, Burlington, MA, USA) and cultivated either with 3T3-J2 FL and KC medium or with the commercially available defined medium Bronchial Epithelial Cell Growth Medium (BEGM™, Lonza, Basel, Switzerland). After two days of confluence, the KC and the BEGM were removed and Cell Combs (from Cell Comb Scratch Assay, Merck-Millipore, Burlington, MA, USA) were used to create two perpendicular scratches across the monolayer. The scratched monolayers were then rinsed with 1x PBS, submerged with KC or BEGM™ medium respectively and placed inside the incubator of Cell Observer Z.1 Microscope (Zeiss, Oberkochen, Germany) to measure progressive wound healing. Images were taken every 10 min for 14 hours (CG and BEGM™ condition) and then every 300 min up to 40 hours (BEGM™ condition). For the quantification, progressive wound healing was assessed each 60 min up to 14 hours and then each 300 min up to 40 hours by calculating the area of wound closure through AxioVision Software (version 4.8).

Trans-epithelial electrical resistance measurement
For Transepithelial electrical resistance (TEER) measurement, human tracheal and bronchial epithelial cells were seeded on Millicell® inserts at 63.200 cells/cm^2 previously coated with FL of lethally irradiated 3T3-J2 cells and cultured in standard submerged condition for 7 days and then in ALI for 30 days. TEER measurements were recorded at days 3, 9, 15, 23, and 29 using a Millicell® ERS-2 voltmeter (Electrical Resistance System, Merck-Millipore, Burlington, MA, USA). The apical surface of cultured epithelia was submerged with epithelial medium (KC) only for the time needed to perform the measurement. Normalization of replicates' resistance values was performed by subtracting the corresponding value of TEER measured in control inserts that did not contain cells. The data were calculated as means ± SD of the measurements performed at each time point.

4. QUANTIFICATION AND STATISTICAL ANALYSIS

The results are presented as mean ± standard deviation (SD). The significance of differences was analysed using Prism 8 software (version 8.4.0, GraphPad Software, San Diego, CA, USA) by Student's unpaired two-sample t-test and $p<0.05$ was considered significant. Details about statistical analyses for each experiment are outlined in the figure legends.

5. KEY RESOURCES TABLE

REAGENT or RESOURCE	SOURCE	IDENTIFIER
Antibodies		
Rabbit polyclonal anti-KERATIN 5	Biolegend	Cat#905504, RRID:AB_2616956
Rabbit polyclonal anti- KERATIN 14	Biolegend	Cat#905301, RRID:AB_2565048
Mouse monoclonal anti- KERATIN 18 (DC10)	Abcam	Cat# ab7797, RRID:AB_306086

Rabbit monoclonal anti- KERATIN 19 (EP1580Y)	Abcam	Cat# ab52625, RRID:AB_2281020
Mouse monoclonal anti-Involucrin	Leica Microsystems	Cat#NCL-INV, RRID:AB_563785
Mouse monoclonal anti-Acetylated Tubulin (6-11b-1)	Sigma	Cat#T7451, RRID:AB_609894
Mouse monoclonal anti-mucin (45 MI)	Progen	Cat#03-16075, RRID:AB_1542395
Rat monoclonal anti-Uteroglobin (394324)	R&D System	Cat#MAB4218, RRID:AB_2183286
Rabbit polyclonal anti-ZO-1	Thermo Fisher Scientific	Cat#40-2200, RRID:AB_2533456
Rabbit polyclonal anti-Ki-67	Abcam	Cat#ab15580, RRID:AB_443209
Rabbit polyclonal anti-p63-alpha	Di Iorio et al., 2005	N/A
Mouse monoclonal anti-14-3-3-Sigma (1.N.6)	Abcam	Cat#ab14123, RRID:AB_300927
Rabbit monoclonal anti-BMI1(D20B7)	Cell Signalling Technology	Cat#6964, RRID:AB_10828713
Rabbit monoclonal anti-SOX2 (D6D9)	Cell Signalling Technology	Cat#3579, RRID:AB_2864411
Mouse monoclonal anti-GAPDH (6C5)	Abcam	Cat# ab8245, RRID:AB_2107448
Mouse monoclonal anti-Vinculin (VIN-11-5)	Sigma-Aldrich	Cat#V4505, RRID:AB_477617
Mouse monoclonal anti-Actin (C4)	Abcam	Cat# ab3280, RRID:AB_303668
Donkey anti-mouse IgG (H+L) Cross-Adsorbed Secondary Antibody, Alexa Fluor™ 488	Thermo Fisher Scientific	Cat# A-21202, RRID:AB_141607
Donkey anti-mouse IgG (H+L) Cross-Adsorbed Secondary Antibody, Alexa Fluor™ 568	Thermo Fisher Scientific	Cat#A-10037, RRID:AB_2534013
Donkey anti-rabbit IgG (H+L) Cross-Adsorbed Secondary Antibody, Alexa Fluor™ 488	Thermo Fisher Scientific	Cat#A-21206, RRID:AB_2535792
Donkey anti-rabbit IgG (H+L) Cross-Adsorbed Secondary Antibody, Alexa Fluor™ 568	Thermo Fisher Scientific	Cat#A10042, RRID:AB_2534017
Goat anti-rat IgG (H+L) 488	Thermo Fisher Scientific	Cat#A-11006, RRID:AB_2534074
Chicken anti-rat IgG-HRP	Santa Cruz Biotechnology	Cat#sc-2956, RRID:AB_639257
Goat anti-mouse IgG H&L (HRP)	Abcam	Cat#ab6789, RRID:AB_955439
Donkey anti-rabbit IgG-HRP	Santa Cruz Biotechnology	Cat#sc-2313, RRID:AB_641181
4′,6-diamidino-2-fenilindolo	Merck	Cat#10236276001
Dako Fluorescence Mountain Medium	Agilent	Cat#S3023
BEGM™ Bronchial Epithelial Cell Growth Medium BulletKit™	Lonza	Cat#CC-3170
Biological samples		
NHBE – Normal Human Bronchial Epithelial Cells	Lonza	Cat#CC-2540
Chemicals		
DMEM High Glucose	Euroclone	Cat#ECB7501L
Ham's F12	Euroclone	Cat#ECB7502L
Fetal bovine serum characterized	Hyclone	Cat#SH30071.03
Donor bovine serum	Thermo Fisher Scientific	Cat#16030-074

L-Glutamine 100X	Euroclone	Cat#ECB3000D
Penicillin-Streptomycin 100X	Euroclone	Cat#ECB3001D
0.25% Trypsin-EDTA 1X	Thermo Fisher Scientific	Cat#25200-072
0.5% Trypsin-EDTA 10X	Thermo Fisher Scientific	Cat#15400-054
Critical commercial assays		
Cell Comb™ Scratch Assay	Merck	Cat#17-10191
Software and Algorithms		
GraphPad Prism 8	GraphPad Software	RRID:SCR_002798
ImageJ	National Institute of Health	RRID:SCR_003070
Image Lab software	Bio-Rad	RRID:SCR_014210

Supplementary video 1. *In vitro* wound closure of AT cells
Wound healing assay performed on a confluent monolayer of AT cells grown in CG or BEGM™ culture condition. Images were taken through live-imaging (Cell Observer®, Zeiss) every 10 min for 14 hours (CG and BEGM™ condition) and then every 300 min up to 40 hours (BEGM™ condition).

Supplementary video 2. Ciliated cells functionality
Video showing a cluster of ciliated cells - detached from the support after 30 days of ALI culture - moving and spinning within the cell culture plate.

References

1. Maina, J.N. (2008). Functional morphology of the avian respiratory system, the lung-air sac system: Efficiency built on complexity. Ostrich *79*, 117–132. 10.2989/OSTRICH.2008.79.2.1.575.
2. Bhutani, V.K. (2012). Pulmonary Gas Exchange. In Manual of Neonatal Respiratory Care (Springer US), pp. 39–47. 10.1007/978-1-4614-2155-9_4.
3. Lawrence, D.A., Branson, B., Oliva, I., and Rubinowitz, A. (2015). The wonderful world of the windpipe: a review of central airway anatomy and pathology. Can Assoc Radiol J *66*, 30–43. 10.1016/j.carj.2014.08.003.
4. Piazza, C., Filauro, M., Dikkers, F.G., Nouraei, S.A.R., Sandu, K., Sittel, C., Amin, M.R., Campos, G., Eckel, H.E., and Peretti, G. (2021). Long-term intubation and high rate of tracheostomy in COVID-19 patients might determine an unprecedented increase of airway stenoses: a call to action from the European Laryngological Society. European Archives of Oto-Rhino-Laryngology *278*, 1–7. 10.1007/s00405-020-06112-6.
5. Soriano, L., Khalid, T., Whelan, D., O'huallachain, N., Redmond, K.C., O'brien, F.J., O'leary, C., and Cryan, S.A. (2021). Development and clinical translation of tubular constructs for tracheal tissue engineering: A review. European Respiratory Review *30*. 10.1183/16000617.0154-2021.
6. Proud, D. (2008). Upper airway viral infections. Pulm Pharmacol Ther *21*, 468–473. 10.1016/j.pupt.2007.06.004.
7. Macchiarini, P. (2006). Primary tracheal tumours. Lancet Oncol *7*, 83–91. 10.1016/S1470-2045(05)70541-6.
8. Adamo, D., Galaverni, G., Genna, V.G., Lococo, F., and Pellegrini, G. (2022). The Growing Medical Need for Tracheal Replacement: Reconstructive Strategies Should Overcome Their Limits. Front Bioeng Biotechnol *0*, 451. 10.3389/FBIOE.2022.846632.

9. Genden, E.M., and Laitman, B.M. (2023). Human Tracheal Transplantation. Transplantation *107*, 1698–1705. 10.1097/TP.0000000000004509.
10. Delaere, P.R., and Van Raemdonck, D. (2019). Commentary: The sobering truth about tracheal regeneration. Journal of Thoracic and Cardiovascular Surgery *159*, 2537–2539. 10.1016/j.jtcvs.2019.10.116.
11. Boazak, E.M., and Auguste, D.T. (2018). Trachea Mechanics for Tissue Engineering Design. ACS Biomater Sci Eng *4*, 1272–1284. 10.1021/acsbiomaterials.7b00738.
12. Gao, M., Zhang, H., Dong, W., Bai, J., Gao, B., Xia, D., Feng, B., Chen, M., He, X., Yin, M., et al. (2017). Tissue-engineered trachea from a 3D-printed scaffold enhances whole-segment tracheal repair. Sci Rep *7*. 10.1038/s41598-017-05518-3.
13. Greaney, A.M., and Niklason, L.E. (2021). The History of Engineered Tracheal Replacements: Interpreting the Past and Guiding the Future. Tissue Eng Part B Rev *27*, 341–352. 10.1089/ten.teb.2020.0238.
14. GonfiOtti, A., Jaus, M.O., Barale, D., Baiguera, S., Comin, C., Lavorini, F., Fontana, G., Sibila, O., Rombolà, G., Jungebluth, P., et al. (2014). The fi rst tissue-engineered airway transplantation: 5-year follow-up results. The Lancet *383*, 238–244. 10.1016/S0140-6736(13)62033-4.
15. Macchiarini, P., Jungebluth, P., Go, T., Asnaghi, M.A., Rees, L.E., Cogan, T.A., Dodson, A., Martorell, J., Bellini, S., Parnigotto, P.P., et al. (2008). Clinical transplantation of a tissue-engineered airway. The Lancet *372*, 2023–2030. 10.1016/S0140-6736(08)61598-6.
16. Elliott, M.J., Butler, C.R., Varanou-Jenkins, A., Partington, L., Carvalho, C., Samuel, E., Crowley, C., Lange, P., Hamilton, N.J., Hynds, R.E., et al. (2017). Tracheal replacement therapy with a stem cell-seeded graft: Lessons from compassionate use application of a GMP-compliant tissue-engineered medicine. Stem Cells Transl Med *6*, 1458–1464. 10.1002/sctm.16-0443.
17. Khalid T, and O'Leary C. (2023). Engineering Large Airways. Adv Exp Med Biol. 2023;1413:121-135. *1413*, 121–135.
18. Grillo, H.C. (2002). Tracheal replacement: a critical review. Ann Thorac Surg *73*, 1995–2004. 10.1016/S0003-4975(02)03564-6.
19. Fishman, J.M., Lowdell, M., and Birchall, M.A. (2014). Stem cell-based organ replacements-Airway and lung tissue engineering. Semin Pediatr Surg *23*. 10.1053/j.sempedsurg.2014.04.002.
20. Lovett, M., Lee, K., Edwards, A., and Kaplan, D.L. (2009). Vascularization Strategies for Tissue Engineering. Tissue Eng Part B Rev *15*, 353. 10.1089/TEN.TEB.2009.0085.
21. Paternoster, J.L., and Vranckx, J.J. (2021). State of the art of clinical applications of Tissue Engineering in 2021. Tissue Eng Part B Rev, 1–76. 10.1089/ten.teb.2021.0017.
22. Den Hondt, M., and Vranckx, J.J. (2017). Reconstruction of defects of the trachea. J Mater Sci Mater Med *28*. 10.1007/s10856-016-5835-x.
23. Varma, R., Marin-Araujo, A.E., Rostami, S., Waddell, T.K., Karoubi, G., Haykal, S., Varma, R., Marin-Araujo, A.E., Rostami, S., Waddell, T.K., et al. (2021). Pre-Clinical Application of Functional Human Induced Pluripotent Stem Cell-Derived Airway Epithelial Grafts. Adv Healthc Mater. *10 (21)*. 10.1101/2021.05.18.444629.
24. Heijink, I.H., Nawijn, M.C., and Hackett, T.L. (2014). Airway epithelial barrier function regulates the pathogenesis of allergic asthma. Clinical and Experimental Allergy *44*, 620–630. 10.1111/cea.12296.
25. Goldfarbmuren, K.C., Jackson, N.D., Sajuthi, S.P., Dyjack, N., Li, K.S., Rios, C.L., Plender, E.G., Montgomery, M.T., Everman, J.L., Bratcher, P.E., et al. (2020). Dissecting the cellular

specificity of smoking effects and reconstructing lineages in the human airway epithelium. Nat Commun *11*. 10.1038/s41467-020-16239-z.
26. Ramirez, R.D., Sheridan, S., Girard, L., Sato, M., Kim, Y., Pollack, J., Peyton, M., Zou, Y., Kurie, J.M., Dimaio, J.M., et al. (2004). Immortalization of Human Bronchial Epithelial Cells in the Absence of Viral Oncoproteins. Cancer Res. *64 (24)*, 9027–9034.
27. Reddel, R.R., Ke, Y., Gerwin, B.I., McMenamin, M.G., Lechner, J.F., Su, R.T., Brash, D.E., Park, J.B., Rhim, J.S., and Harris, C.C. (1988). Transformation of Human Bronchial Epithelial Cells by Infection with SV40 or Adenovirus-12 SV40 Hybrid Virus, or Transfection via Strontium Phosphate Coprecipitation with a Plasmid Containing SV40 Early Region Genes. Cancer Res *48*, 1904–1909.
28. Walters, M.S., Gomi, K., Ashbridge, B., Moore, M.A.S., Arbelaez, V., Heldrich, J., Ding, B., Rafii, S., Staudt, M.R., and Crystal, R.G. (2013). Generation of a human airway epithelium derived basal cell line with multipotent differentiation capacity. Respir Res. *14 (1)*, 26–30.
29. Araya, J., Cambier, S., Markovics, J.A., Wolters, P., Jablons, D., Hill, A., Finkbeiner, W., Jones, K., Broaddus, V.C., Sheppard, D., et al. (2007). Squamous metaplasia amplifies pathologic epithelial-mesenchymal interactions in COPD patients. Journal of Clinical Investigation *117*, 3551–3562. 10.1172/JCI32526.
30. Gray, T.E., Guzman, K., Davis, C.W., Abdullah, L.H., and Nettesheim, P. (1996). Mucociliary Differentiation of Serially Passaged Normal Human Tracheobronchial Epithelial Cells. Am J Respir Cell Mol Biol *14*, 104–112. 10.1165/ajrcmb.14.1.8534481.
31. Widdicombe, J.H., Sachs, L.A., Morrow, J.L., and Finkbeiner, W.E. (2005). Expansion of cultures of human tracheal epithelium with maintenance of differentiated structure and function. Biotechniques *39*, 249–255. 10.2144/05392RR02.
32. Bukowy-Bieryłło, Z. (2021). Long-term differentiating primary human airway epithelial cell cultures: how far are we? Cell Communication and Signaling *19*, 1–18. 10.1186/s12964-021-00740-z.
33. Butler, C.R., Hynds, R.E., Gowers, K.H.C., Do, D., Lee, H., Brown, J.M., Crowley, C., Teixeira, V.H., Smith, C.M., Urbani, L., et al. (2016). Rapid Expansion of Human Epithelial Stem Cells Suitable for Airway Tissue Engineering. *194*, 156–168. 10.1164/rccm.201507-1414OC.
34. Pellegrini, G., Ardigò, D., Milazzo, G., Iotti, G., Guatelli, P., Pelosi, D., and De Luca, M. (2018). Navigating Market Authorization: The Path Holoclar Took to Become the First Stem Cell Product Approved in the European Union. Stem Cells Transl Med *7*, 146–154. 10.1002/sctm.17-0003.
35. De Luca, M., Pellegrini, G., and Green, H. (2006). Regeneration of squamous epithelia from stem cells of cultured grafts. Regenerative Med *1*, 45–57. 10.2217/17460751.1.1.45.
36. De Luca, M., Aiuti, A., Cossu, G., Parmar, M., Pellegrini, G., and Robey, P.G. (2019). Advances in stem cell research and therapeutic development. Nat Cell Biol *21*, 801–811. 10.1038/s41556-019-0344-z.
37. Maurizi, E., Adamo, D., Magrelli, F.M., Galaverni, G., Attico, E., Merra, A., Maffezzoni, M.B.R., Losi, L., Genna, V.G., Sceberras, V., et al. (2021). Regenerative Medicine of Epithelia: Lessons From the Past and Future Goals. Front Bioeng Biotechnol *9*. 10.3389/fbioe.2021.652214.
38. Pellegrini, G., Rama, P., Matuska, S., Lambiase, A., Bonini, S., Pocobelli, A., Colabelli, R.G., Spadea, L., Fasciani, R., Balestrazzi, E., et al. (2013). Biological parameters determining the clinical outcome of autologous cultures of limbal stem cells. Regenerative Med *8*, 553–567. 10.2217/rme.13.43.
39. Pellegrini, G., Ranno, R., Stracuzzi, G., Bondanza, S., Guerra, L., Zambruno, G., Micali, G., and De Luca, M. (1999). The control of epidermal stem cells (holoclones) in the treatment of

massive full-thickness burns with autologous keratinocytes cultured on fibrin. Transplantation *68*, 868–879.
40. Di Iorio, E., Barbaro, V., Ferrari, S., Ortolani, C., De Luca, M., and Pellegrini, G. (2006). Q-FIHC: Quantification of fluorescence immunohistochemistry to analyse p63 isoforms and cell cycle phases in human limbal stem cells. Microsc Res Tech *69*, 983–991. 10.1002/jemt.20375.
41. Hynds, R.E., Bonfanti, P., and Janes, S.M. (2018). Regenerating human epithelia with cultured stem cells: feeder cells, organoids and beyond. EMBO Mol Med *10*, 139–150. 10.15252/emmm.201708213.
42. Rama, P., Matuska, S., Paganoni, G., Spinelli, A., De Luca, M., and Pellegrini, G. (2010). Limbal Stem-Cell Therapy and Long-Term Corneal Regeneration. New England Journal of Medicine *363*, 147–155. 10.1056/nejmoa0905955.
43. Hirsch, T., Rothoeft, T., Teig, N., Bauer, J.W., Pellegrini, G., De Rosa, L., Scaglione, D., Reichelt, J., Klausegger, A., Kneisz, D., et al. (2017). Regeneration of the entire human epidermis using transgenic stem cells. Nature *551*, 327–332. 10.1038/nature24487.
44. Pellegrini, G., Traverso, C.E., Franzi, A.T., Zingirian, M., Cancedda, R., and De Luca, M. (1997). Long-term restoration of damaged corneal surfaces with autologous cultivated corneal epithelium. Lancet *349*, 990–993. 10.1016/S0140-6736(96)11188-0.
45. Genna, V.G., Adamo, D., Galaverni, G., Lepore, F., Boraldi, F., Quaglino, D., Lococo, F., and Pellegrini, G. (2023). Validation of airway porcine epithelial cells as an alternative to human in vitro preclinical studies. Sci Rep *13*, 16290. 10.1038/S41598-023-43284-7.
46. Zaragosi, L.E., Deprez, M., and Barbry, P. (2020). Using single-cell RNA sequencing to unravel cell lineage relationships in the respiratory tract. Biochem Soc Trans *48*, 327–336. 10.1042/BST20191010.
47. Rheinwatd, J.G., and Green, H. (1975). Seria cultivation of strains of human epidemal keratinocytes: the formation keratinizin colonies from single cell is. Cell *6*, 331–343. 10.1016/S0092-8674(75)80001-8.
48. Gallico G., O.C.NE. (1985). Cultured Epithelium as a Skin Substitute. Clin Plast Surg. *12 (2)*, 149–157.
49. Corradini, F., Zattoni, M., Barbagli, G., Bianchi, G., Giovanardi, M., Serafini, C., G. Genna, V., Ribbene, A., Balò, S., Fidanza, F., et al. (2016). Comparative Assessment of Cultures from Oral and Urethral Stem Cells for Urethral Regeneration. Curr Stem Cell Res Ther *11*, 643–651. 10.2174/1574888X10666150902094644.
50. Pellegrini, G., Golisano, O., Paterna, P., Lambiase, A., Bonini, S., Rama, P., and De Luca, M. (1999). Location and Clonal Analysis of Stem Cells and Their Differentiated Progeny in the Human Ocular Surface. J Cell Biol *145*, 769–782.
51. Barbaro, V., Testa, A., Di Iorio, E., Mavilio, F., Pellegrini, G., and De Luca, M. (2007). C/EBPδ regulates cell cycle and self-renewal of human limbal stem cells. Journal of Cell Biology *177*, 1037–1049. 10.1083/jcb.200703003.
52. Dovey, J.S., Zacharek, S.J., Kim, C.F., and Lees, J.A. (2008). Bmi1 is critical for lung tumorigenesis and bronchioalveolar stem cell expansion. Proc Natl Acad Sci U S A. *105 (33)*, 11857–11862.
53. Takahashi, K., and Yamanaka, S. (2006). Induction of Pluripotent Stem Cells from Mouse Embryonic and Adult Fibroblast Cultures by Defined Factors. Cell *126*, 663–676. 10.1016/j.cell.2006.07.024.
54. Daniely, Y., Liao, G., Dixon, D., Linnoila, R.I., Lori, A., Randell, S.H., Oren, M., and Jetten, A.M. (2004). Critical role of p63 in the development of a normal esophageal and tracheobronchial epithelium. Am J Physiol Cell Physiol *287*, 171–181. 10.1152/ajpcell.00226.2003.

55. Yu, P., Clayman, G.L., and Walsh, G.L. (2006). Human tracheal reconstruction with a composite radial forearm free flap and prosthesis. Annals of Thoracic Surgery *81*, 714–716. 10.1016/j.athoracsur.2004.12.009.
56. Garcıá, S.R., Deprez, M., Lebrigand, K., Cavard, A., Paquet, A., Arguel, M.J., Magnone, V., Truchi, M., Caballero, I., Leroy, S., et al. (2019). Novel dynamics of human mucociliary differentiation revealed by single-cell RNA sequencing of nasal epithelial cultures. Development (Cambridge) *146*. 10.1242/dev.177428.
57. Gerovac, B.J., Valencia, M., Baumlin, N., Salathe, M., Conner, G.E., and Fregien, N.L. (2014). Submersion and hypoxia inhibit ciliated cell differentiation in a Notch-dependent manner. Am J Respir Cell Mol Biol *51*, 516–525. 10.1165/rcmb.2013-0237OC.
58. Ostrowski, L.E., and Nettesheim, P. (1995). Inhibition of ciliated cell differentiation by fluid submersion. Exp Lung Res. *21 (6)*, 957–970.
59. De Jong, P.M., Van Sterkenburg, M.A.J.A., Hesseling, S.C., Kempenaar, J.A., Mulder, A.A., Mommaas, A.M., Dijkman, J.H., and Ponec, M. (1994). Ciliogenesis in Human Bronchial Epithelial Cells Cultured at the Air-Liquid Interface. Am. J. Respir. Cell Mol. Biol *10*, 271–277.
60. Kumar, P.A., Hu, Y., Yamamoto, Y., Hoe, N.B., Wei, T.S., Mu, D., Sun, Y., Joo, L.S., Dagher, R., Zielonka, E.M., et al. (2011). Distal airway stem cells yield alveoli in vitro and during lung regeneration following H1N1 influenza infection. Cell *147*, 525–538. 10.1016/j.cell.2011.10.001.
61. Barrandon, Y., and Green, H. (1987). Three clonal types of keratinocyte with different capacities for multiplication. Proc. Nati. Acad. Sci. USA *84*, 2302–2306.
62. Ragazzini, R., Boeing, S., Zanieri, L., Green, M., D'Agostino, G., Bartolovic, K., Agua-Doce, A., Greco, M., Watson, S.A., Batsivari, A., et al. (2023). Defining the identity and the niches of epithelial stem cells with highly pleiotropic multilineage potency in the human thymus. Dev Cell. 10.1016/j.devcel.2023.08.017.
63. Romagnoli, G., De Luca, M., Faranda, F., Bandelloni, R., Franzi, A.T., Cataliotti, F., and Cancedda, R. (1990). Treatment of Posterior Hypospadias by the Autologous Graft of Cultured Urethral Epithelium. N Engl J Med. *323*, 527–530. 10.1056/NEJM199008233230806.
64. De Luca, M., Albanese, E., Megna, M., Cancedda, R., Mangiante, P., Cadoni, A., and Franzi, A. (1990). Evidence that human oral epithelium reconstituted in vitro and transplanted onto patients with defects in the oral mucosa retains properties of the original donor site. Transplantation *50 (3)*, 454–459.
65. Enzo, E., Secone Seconetti, A., Forcato, M., Tenedini, E., Polito, M.P., Sala, I., Carulli, S., Contin, R., Peano, C., Tagliafico, E., et al. (2021). Single-keratinocyte transcriptomic analyses identify different clonal types and proliferative potential mediated by FOXM1 in human epidermal stem cells. Nat Commun *12*. 10.1038/s41467-021-22779-9.
66. Dellambra, E., Golisano, O., Bondanza, S., Siviero, E., Lacal, P., Molinari, M., D'atri, S., and De Luca, M. (2000). Downregulation of 14-3-3 Prevents Clonal Evolution and Leads to Immortalization of Primary Human Keratinocytes. J Cell Biol *149*, 1117–1129.
67. Pellegrini, G., Dellambra, E., Golisano, O., Martinelli, E., Fantozzi, I., Bondanza, S., Ponzin, D., McKeon, F., and De Luca, M. (2001). P63 Identifies Keratinocyte Stem Cells. Proc Natl Acad Sci U S A *98*, 3156–3161. 10.1073/pnas.061032098.
68. Rochat, A., and Barrandon, Y. (2004). Regeneration of Epidermis from Adult Keratinocyte Stem Cells 10.1016/B978-0-12-436643-5.50159-0.
69. Pellegrini, G., Rama, P., Di Rocco, A., Panaras, A., and De Luca, M. (2014). Concise review: Hurdles in a successful example of limbal stem cell-based regenerative medicine. Stem Cells *32*, 26–34. 10.1002/stem.1517.

70. Pellegrini, G., Lambiase, A., Macaluso, C., Pocobelli, A., Deng, S., Cavallini, G.M., Esteki, R., and Rama, P. (2016). From discovery to approval of an advanced therapy medicinal product-containing stem cells, in the EU. Regenerative Med *11*, 407–420. 10.2217/rme-2015-0051.
71. Fulcher, M.L., Gabriel, S.E., Olsen, J.C., Tatreau, J.R., Gentzsch, M., Livanos, E., Saavedra, M.T., Salmon, P., and Randell, S.H. (2009). Novel human bronchial epithelial cell lines for cystic fibrosis research. Am J Physiol Lung Cell Mol Physiol *296*, 82–91. 10.1152/ajplung.90314.2008.
72. Yankaskas, J.R., Haizlip, J.E., Conrad, M., Koval, D., Lazarowski, E., Paradiso, A.M., Rinehart, C.A., Sarkadi, B., Schlegel, R., and Boucher, R.C. (1993). Papilloma virus immortalized tracheal epithelial cells retain a well- differentiated phenotype. Am J Physiol Cell Physiol *264*. 10.1152/ajpcell.1993.264.5.c1219.
73. Lehman, T.A., Modali, R., Boukamp, P., Stanek, J., Bennett, W.P., Welsh, J.A., Metcalf, R.A., Stampfer, M.R., Fusenig, N., Rogan, E.M., et al. (1993). Accelerated paper p53 Mutations in human immortalized epithelial cell lines. Carcinogenesis *14*, 833–839.
74. Lynn Allen-Hoffmann, B., Schlosser, S.J., R Ivarie, C.A., Sattler, C.A., Meisner, L.F., and O, S.L. (2000). Normal Growth and Differentiation in a Spontaneously Immortalized Near-Diploid Human Keratinocyte Cell Line, NIKS. J Invest Dermatol. *114 (3)*, 444–455.
75. Chapman, S., Liu, X., Meyers, C., Schlegel, R., and Mcbride, A.A. (2010). Technical advance Human keratinocytes are efficiently immortalized by a Rho kinase inhibitor. *120*, 14–21. 10.1172/JCI42297DS1.
76. Suprynowicz, F.A., Upadhyay, G., Krawczyk, E., Kramer, S.C., Hebert, J.D., Liu, X., Yuan, H., Cheluvaraju, C., Clapp, P.W., Boucher, R.C., et al. (2012). Conditionally reprogrammed cells represent a stem-like state of adult epithelial cells. Proc Natl Acad Sci U S A *109*, 20035–20040. 10.1073/pnas.1213241109.
77. Horani, A., Ferkol, T.W., Shoseyov, D., Wasserman, M.G., Oren, Y.S., Kerem, B., Amirav, I., Cohen-Cymberknoh, M., Dutcher, S.K., Brody, S.L., et al. (2013). LRRC6 Mutation Causes Primary Ciliary Dyskinesia with Dynein Arm Defects. PLoS One *8*. 10.1371/journal.pone.0059436.
78. Liu, X., Ory, V., Chapman, S., Yuan, H., Albanese, C., Kallakury, B., Timofeeva, O.A., Nealon, C., Dakic, A., Simic, V., et al. (2012). ROCK inhibitor and feeder cells induce the conditional reprogramming of epithelial cells. American Journal of Pathology *180*, 599–607. 10.1016/j.ajpath.2011.10.036.
79. Mou, H., Vinarsky, V., Tata, P.R., Brazauskas, K., Choi, S.H., Crooke, A.K., Zhang, B., Solomon, G.M., Turner, B., Bihler, H., et al. (2016). Dual SMAD Signaling Inhibition Enables Long-Term Expansion of Diverse Epithelial Basal Cells. Cell Stem Cell *19*, 217–231. 10.1016/j.stem.2016.05.012.
80. Awatade, N.T., Wong, S.L., Capraro, A., Pandzic, E., Slapetova, I., Zhong, L., Turgutoglu, N., Fawcett, L.K., Whan, R.M., Jaffe, A., et al. (2021). Significant functional differences in differentiated Conditionally Reprogrammed (CRC)- and Feeder-free Dual SMAD inhibited-expanded human nasal epithelial cells. Journal of Cystic Fibrosis *20*, 364–371. 10.1016/j.jcf.2020.12.019.
81. He, X.C., Zhang, J., Tong, W.G., Tawfik, O., Ross, J., Scoville, D.H., Tian, Q., Zeng, X., He, X., Wiedemann, L.M., et al. (2004). BMP signaling inhibits intestinal stem cell self-renewal through suppression of Wnt-β-catenin signaling. Nat Genet *36*, 1117–1121. 10.1038/ng1430.
82. Kobielak, K., Stokes, N., De La Cruz, J., Polak, L., and Fuchs, E. (2007). Loss of a quiescent niche but not follicle stem cells in the absence of bone morphogenetic protein signaling. Proc Natl Acad Sci U S A. *104 (24)*, 10063–10068.

83. Oshimori, N., and Fuchs, E. (2012). Paracrine TGF-β signaling counterbalances BMP-mediated repression in hair follicle stem cell activation. Cell Stem Cell *10*, 63–75. 10.1016/j.stem.2011.11.005.
84. Raldine Guasch, G., Schober, M., Pasolli, H.A., Conn, E.B., Polak, L., and Fuchs, E. (2007). Article Loss of TGFb Signaling Destabilizes Homeostasis and Promotes Squamous Cell Carcinomas in Stratified Epithelia. Cancer Cell *12 (4)*, 313–327. 10.1016/j.ccr.2007.08.020.
85. Blanpain, C., Horsley, V., and Fuchs, E. (2007). Epithelial Stem Cells: Turning over New Leaves. Cell *128 (3)*, 445–458.
86. Gilpin, S.E., Charest, J.M., Ren, X., Tapias, L.F., Wu, T., Evangelista-Leite, D., Mathisen, D.J., and Ott, H.C. (2016). Regenerative potential of human airway stem cells in lung epithelial engineering. Biomaterials *108*, 111–119. 10.1016/j.biomaterials.2016.08.055.
87. Watt, F.M., and Jensen, K.B. (2009). Epidermal stem cell diversity and quiescence. EMBO Mol Med *1*, 260–267. 10.1002/emmm.200900033.
88. Sacchetti, M., Rama, P., Bruscolini, A., and Lambiase, A. (2018). Limbal stem cell transplantation: Clinical results, limits, and perspectives. Stem Cells Int *2018*. 10.1155/2018/8086269.
89. Blanpain, C., and Fuchs, E. (2009). Epidermal homeostasis: A balancing act of stem cells in the skin. Nat Rev Mol Cell Biol *10*, 207–217. 10.1038/nrm2636.
90. Pellegrini, G., Rama, P., and De Luca, M. (2011). Vision from the right stem. Trends Mol Med *17*, 1–7. 10.1016/j.molmed.2010.10.003.
91. Hong, K.U., Reynolds, S.D., Watkins, S., Fuchs, E., and Stripp, B.R. (2004). Basal Cells Are a Multipotent Progenitor Capable of Renewing the Bronchial Epithelium. Am J Pathol. *164 (2)*, 577–588.
92. Rock, J.R., Onaitis, M.W., Rawlins, E.L., Lu, Y., Clark, C.P., Xue, Y., Randell, S.H., and Hogan, B.L.M. (2009). Basal cells as stem cells of the mouse trachea and human airway epithelium. Proc Natl Acad Sci U S A. *106 (31)*, 12771–12775.
93. Di Iorio, E., Barbaro, V., Ferrari, S., Ortolani, C., De Luca, M., and Pellegrini, G. (2006). Q-FIHC: Quantification of fluorescence immunohistochemistry to analyse p63 isoforms and cell cycle phases in human limbal stem cells. Microsc Res Tech *69*, 983–991. 10.1002/jemt.20375.
94. Rochat, A., Kobayashi, K., and Barrandon, Y. (1994). Location of Stem Cells of Human Hair Follicles by Clonal Analysis. Cell *76*, 1063–1073.
95. Senoo, M., Pinto, F., Crum, C.P., and McKeon, F. (2007). p63 Is Essential for the Proliferative Potential of Stem Cells in Stratified Epithelia. Cell *129*, 523–536. 10.1016/j.cell.2007.02.045.
96. Li, W., Sabater, A.L., Chen, Y.T., Hayashida, Y., Chen, S.Y., He, H., and Tseng, S.C.G. (2007). A novel method of isolation, preservation, and expansion of human corneal endothelial cells. Invest Ophthalmol Vis Sci *48*, 614–620. 10.1167/iovs.06-1126.
97. Candi, E., Dinsdale, D., Rufini, A., Salomoni, P., Knight, R.A., Mueller, M., Krammer, P.H., and Melino, G. (2007). TAp63 and ΔNp63 in cancer and epidermal development. Cell Cycle *6*, 274–284. 10.4161/cc.6.3.3797.
98. Park, I., Morrison, S.J., and Clarke, M.F. (2004). Bmi1, stem cells, and senescence regulation. J Clin Invest *113*, 175–179. 10.1172/JCI200420800.Many.
99. Molofsky, A. V., He, S., Bydon, M., Morrison, S.J., and Pardal, R. (2005). Bmi-1 promotes neural stem cell self-renewal and neural development but not mouse growth and survival by repressing the p16Ink4a and p19 Arf senescence pathways. Genes Dev *19*, 1432–1437. 10.1101/gad.1299505.

100. Gontan, C., Munck, A. De, Vermeij, M., Grosveld, F., Tibboel, D., and Rottier, R. (2008). Sox2 is important for two crucial processes in lung development : Branching morphogenesis and epithelial cell differentiation. Dev Biol. *317*, 296–309. 10.1016/j.ydbio.2008.02.035.
101. Hashimoto, S., Chen, H., Que, J., Brockway, B.L., Drake, J.A., Snyder, J.C., Randell, S.H., and Stripp, B.R. (2012). β-catenin-SOX2 signaling regulates the fate of developing airway epithelium. Development *139*, 932–942. 10.1242/jcs.092734.
102. Tompkins, D.H., Besnard, V., Lange, A.W., Keiser, A.R., Wert, S.E., Bruno, M.D., and Whitsett, J.A. (2011). Sox2 activates cell proliferation and differentiation in the respiratory epithelium. Am J Respir Cell Mol Biol *45*, 101–110. 10.1165/rcmb.2010-0149OC.
103. Basil, M.C., Katzen, J., Engler, A.E., Guo, M., Herriges, M.J., Kathiriya, J.J., Windmueller, R., Ysasi, A.B., Zacharias, W.J., Chapman, H.A., et al. (2020). The Cellular and Physiological Basis for Lung Repair and Regeneration: Past, Present, and Future. Cell Stem Cell *26*, 482–502. 10.1016/j.stem.2020.03.009.
104. Van Keymeulen, A., and Blanpain, C. (2012). Tracing epithelial stem cells during development, homeostasis, and repair. Journal of Cell Biology *197*, 575–584. 10.1083/jcb.201201041.
105. Rawlins, E.L., Okubo, T., Xue, Y., Brass, D.M., Auten, R.L., Hasegawa, H., Wang, F., and Hogan, B.L.M. (2009). The Role of Scgb1a1+ Clara Cells in the Long-Term Maintenance and Repair of Lung Airway, but Not Alveolar, Epithelium. Cell Stem Cell *4*, 525–534. 10.1016/j.stem.2009.04.002.
106. Engelhardt, J.F. (2001). Stem cell niches in the mouse airway. Am J Respir Cell Mol Biol *24*, 649–652. 10.1165/ajrcmb.24.6.f206.
107. Zuo, W.L., Shenoy, S.A., Li, S., O'Beirne, S.L., Strulovici-Barel, Y., Leopold, P.L., Wang, G., Staudt, M.R., Walters, M.S., Mason, C., et al. (2018). Ontogeny and biology of human small airway epithelial club cells. Am J Respir Crit Care Med *198*, 1375–1388. 10.1164/rccm.201710-2107OC.
108. Okuda, K., Chen, G., Subramani, D.B., Wolf, M., Gilmore, R.C., Kato, T., Radicioni, G., Kesimer, M., Chua, M., Dang, H., et al. (2019). Localization of secretory mucins MUC5AC and MUC5B in normal/healthy human airways. Am J Respir Crit Care Med *199*, 715–727. 10.1164/rccm.201804-0734OC.
109. Kouznetsova, I., Chwieralski, C.E., Bälder, R., Hinz, M., Braun, A., Krug, N., and Hoffmann, W. (2007). Induced trefoil factor family 1 expression by trans-differentiating Clara cells in a murine asthma model. Am J Respir Cell Mol Biol *36*, 286–295. 10.1165/rcmb.2006-0008OC.
110. Chen, G., Korfhagen, T.R., Xu, Y., Kitzmiller, J., Wert, S.E., Maeda, Y., Gregorieff, A., Clevers, H., and Whitsett, J.A. (2009). SPDEF is required for mouse pulmonary goblet cell differentiation and regulates a network of genes associated with mucus production. Journal of Clinical Investigation *119*, 2914–2924. 10.1172/JCI39731.
111. Tata, P.R., Mou, H., Pardo-Saganta, A., Zhao, R., Prabhu, M., Law, B.M., Vinarsky, V., Cho, J.L., Breton, S., Sahay, A., et al. (2013). Dedifferentiation of committed epithelial cells into stem cells in vivo. Nature *503*, 218–223. 10.1038/nature12777.
112. Montoro, D.T., Haber, A.L., Biton, M., Vinarsky, V., Lin, B., Birket, S.E., Yuan, F., Chen, S., Leung, H.M., Villoria, J., et al. (2018). A revised airway epithelial hierarchy includes CFTR-expressing ionocytes. Nature *560*, 319–324. 10.1038/s41586-018-0393-7.